

Day-ahead scheduling of energy hubs with parking lots for electric vehicles considering uncertainties

A. Rezaee Jordehi^{a,1}, Mohammad Sadegh Javadi², João P. S. Catalão^{2,3}

^a*Department of Electrical Engineering, Rasht Branch, Islamic Azad University, Rasht, Iran*

²*INESC TEC, Porto, Portugal*

³*Faculty of Engineering of the University of Porto, Porto, Portugal*

Abstract- Energy hubs (EHs) are units in which multiple energy carriers are converted, conditioned and stored to simultaneously supply different forms of energy demands. In this research, the objective is to develop a new stochastic model for unit commitment in EHs including an intelligent electric vehicle (EV) parking lot, boiler, photovoltaic (PV) module, fuel cell, absorption chiller, electric heat pump, electric/thermal/cooling storage systems, with electricity and natural gas (NG) as inputs and electricity, heat, cooling and NG as demands. The uncertainties of demands, PV power and initial energy of EV batteries are modeled with Monte Carlo Simulation. The effect of demand response and demand participation factors as well as effect of EVs and storage systems on EH operation are investigated. The results indicate that thermal demand response is more effective than electric and cooling demand response; as it decreases EH operation cost by 12%, while electric demand response and cooling demand response decrease it respectively by 9.3% and 4.2%. The results show that at low electric/thermal/cooling demand participation factors, an increase in participation factor sharply decreases EH operation cost, while the same amount of increase at higher participation factors leads to a smaller decrease in operation cost. The results also indicate that thermal storage system and cooling storage system have significant effect on reduction of EH operation cost, while the effect of electric storage system is trivial.

Keywords: energy hubs; optimisation; unit commitment; electric vehicles; uncertainty

¹Corresponding author at: Rasht Branch, Islamic Azad University, Rasht, Iran.
E-mail address: ahmadrezaeejordehi@gmail.com.

Nomenclature

Acronyms

EH	Energy hub
UC	Unit commitment
MCS	Monte Carlo Simulation
DR	Demand response
CHP	Combined heat and power
CCHP	Combined cooling heat and power
FC	Fuel cell
ESS	Electric storage system
BSS	Battery storage system
TSS	Thermal storage system
CSS	Cooling storage system
P2G	Power to gas (storage)
V2G	Vehicle to grid
PV	Photovoltaic
WT	Wind turbine
NG	Natural gas
MILP	Mixed-integer linear programming
EHP	Electric heat pump
EV	Electric vehicle
COP	Coefficient of performance
TOU	Time of use
EDPF	Electric demand participation factor
TDPF	Thermal demand participation factor
CDPF	Cooling demand participation factor

Indices

t	Index of time
s	Index of scenarios
ev	Index of EVs

Sets

UTS_{ev}	Unavailability times set for ev th EV
------------	---

Parameters

$\pi_{grid,t}$	Price of purchased power from grid at time t
pr_s	Probability of scenario s
$P_{grid,max}$	Maximum importable power from grid
$\pi_{NG,t}$	Price of purchased NG at time t
$P_{NG,max}$	Maximum importable NG from grid
$D_{e,t,s}$	Electric power demand at time t and scenario s
$D_{h,t,s}$	Thermal power demand at time t and scenario s
$D_{c,t,s}$	Cooling power demand at time t and scenario s
$D_{NG,t,s}$	NG demand at time t and scenario s
$PV_{t,s,max}$	Available PV power at time t and scenario s
eff_{TF}	Efficiency of transformer
eff_{conv}	Efficiency of PV's converter
VLL_e	Value of lost electric load
VLL_h	Value of lost thermal load
VLL_c	Value of lost cooling load

$C_{AC,min}$	Minimum cooling power of absorption chiller
$C_{AC,max}$	Maximum cooling power of absorption chiller
COP_{AC}	COP of absorption chiller
RU_{AC}	Ramp-up rate limit of absorption chiller
RD_{AC}	Ramp-down rate limit of absorption chiller
SU_{AC}	Start-up cost of absorption chiller
SD_{AC}	Shut-down cost of absorption chiller
$H_{EHP,min}$	Minimum thermal power of EHP
$H_{EHP,max}$	Maximum thermal power of EHP
$C_{EHP,min}$	Minimum cooling power of EHP
$C_{EHP,max}$	Maximum cooling power of EHP
$COP_{EHP,h}$	Thermal COP of EHP
$COP_{EHP,c}$	Cooling COP of EHP
$RU_{EHP,h}$	Heat ramp-up rate limit of EHP
$RD_{EHP,h}$	Heat ramp-down rate limit of EHP
$RU_{EHP,c}$	Cooling ramp-up rate limit of EHP
$RD_{EHP,c}$	Cooling ramp-down rate limit of EHP
SU_{EHP}	Start-up cost of EHP
SD_{EHP}	Shut-down cost of EHP
eff_{boil}	Efficiency of boiler
RU_{boil}	Ramp-up rate limit of boiler
RD_{boil}	Ramp-down rate limit of boiler
SU_{boil}	Start-up cost of boiler
SD_{boil}	Shut-down cost of boiler
$H_{boil,min}$	Minimum heat of boiler
$H_{boil,max}$	Maximum heat of boiler
$eff_{P,FC}$	Power efficiency of FC
$eff_{H,FC}$	Heat efficiency of FC
$RU_{P,FC}$	Electric ramp-up rate limit of FC
$RD_{P,FC}$	Electric ramp-down rate limit of FC
$RU_{H,FC}$	Thermal ramp-up rate limit of FC
$RD_{H,FC}$	Thermal ramp-down rate limit of FC
SU_{FC}	Start-up cost of FC
SD_{FC}	Shut-down cost of FC
$P_{FC,min}$	Minimum electric power of FC
$P_{FC,max}$	Maximum electric power of FC
$H_{FC,min}$	Minimum thermal power of FC
$H_{FC,max}$	Maximum thermal power of FC
$eff_{BSS,ch}$	Charging efficiency of BSS
$eff_{BSS,dch}$	Discharging efficiency of BSS
RC_{BSS}	Replacement cost of BSS
$TCDC_{BSS}$	Total charge/discharge capacity of BSS
SLF_{BSS}	Storage loss factor of BSS
$E_{BSS,ini}$	Initial energy of BSS
$E_{BSS,min}$	Minimum allowed energy of BSS
$E_{BSS,max}$	Maximum allowed energy of BSS
$Pch_{BSS,min}$	Minimum allowed charging power of BSS
$Pch_{BSS,max}$	Maximum allowed charging power of BSS
$Pdch_{BSS,min}$	Minimum allowed discharging power of BSS
$Pdch_{BSS,max}$	Maximum allowed discharging power of BSS
$eff_{TSS,ch}$	Charging efficiency of TSS

$eff_{TSS,dch}$	Discharging efficiency of TSS
RC_{TSS}	Replacement cost of TSS
$TCDC_{TSS}$	Total charge/discharge capacity of TSS
SLF_{TSS}	Storage loss factor of TSS
$E_{TSS,ini}$	Initial energy of TSS
$E_{TSS,min}$	Minimum allowed energy of TSS
$E_{TSS,max}$	Maximum allowed energy of TSS
$Hch_{TSS,min}$	Minimum charging power of TSS
$Hch_{TSS,max}$	Maximum charging power of TSS
$Hdch_{TSS,min}$	Minimum discharging power of TSS
$Hdch_{TSS,max}$	Maximum discharging power of TSS
COP_{CSS}	COP of CSS charging
$eff_{CSS,dch}$	Discharging efficiency of CSS
RC_{CSS}	Replacement cost of CSS
$TCDC_{CSS}$	Total charge/discharge capacity of CSS
SLF_{CSS}	Storage loss factor of CSS
$E_{CSS,ini}$	Initial energy of CSS
$E_{CSS,min}$	Minimum allowed energy of CSS
$E_{CSS,max}$	Maximum allowed energy of CSS
$Pch_{CSS,min}$	Minimum allowed charging power of CSS
$Pch_{CSS,max}$	Maximum allowed charging power of CSS
$Pdch_{CSS,min}$	Minimum allowed discharging power of CSS
$Pdch_{CSS,max}$	Maximum allowed discharging power of CSS
$eff_{ev,ch}$	Charging efficiency of ev th EV
$eff_{ev,dch}$	Discharging efficiency of ev th EV
RC_{ev}	Replacement cost of ev th EV
$TCDC_{ev}$	Total charge/discharge capacity of ev th EV
SLF_{ev}	Storage loss factor of ev th EV
$E_{ev,ini,s}$	Initial energy of ev th EV at scenario s
$E_{ev,min}$	Minimum allowed energy of ev th EV
$E_{ev,max}$	Maximum allowed energy of ev th EV
$Pch_{ev,min}$	Minimum allowed charging power of ev th EV
$Pch_{ev,max}$	Maximum allowed charging power of ev th EV
$Pdch_{ev,min}$	Minimum allowed discharging power of ev th EV
$Pdch_{ev,max}$	Maximum allowed discharging power of ev th EV
$DPF_{e,up}$	Electric demand participation factor for shift-up
$DPF_{e,down}$	Electric demand participation factor for shift-down
$DPF_{h,up}$	Thermal demand participation factor for shift-up
$DPF_{h,down}$	Thermal demand participation factor for shift-down
$DPF_{c,up}$	Cooling demand participation factor for shift-up
$DPF_{c,down}$	Cooling demand participation factor for shift-down
DRI_e	Demand response incentive for electric demand
DRI_h	Demand response incentive for thermal demand
DRI_c	Demand response incentive for cooling demand
$P_{shed,t,max}$	Maximum power shed at time t
$H_{shed,t,max}$	Maximum thermal shed at time t
$C_{shed,t,max}$	Maximum cooling demand shed at time t

Variables

OC	Expected operation cost of EH
OC_s	Operation cost of EH at scenario s

$P_{grid,t,s}$	Imported power from grid at time t and scenario s
$P_{NG,t,s}$	Imported NG from grid at time t and scenario s
$PV_{t,s}$	Injected PV power to EH at time t and scenario s
$P_{shed,t,s}$	Electric demand shed at time t and scenario s
$H_{shed,t,s}$	Thermal demand shed at time t and scenario s
$C_{shed,t,s}$	Cooling demand shed at time t and scenario s
$d_{BSS,s}$	Degradation cost of BSS at scenario s
$d_{TSS,s}$	Degradation cost of TSS at scenario s
$d_{CSS,s}$	Degradation cost of CSS at scenario s
$d_{fleet,s}$	Degradation cost of EV fleet at scenario s
DRC_s	Demand response cost at scenario s
$DRC_{e,s}$	Total incentive paid to responsive electric demands at scenario s
$DRC_{h,s}$	Total incentive paid to responsive thermal demands at scenario s
$DRC_{c,s}$	Total incentive paid to responsive cooling demands at scenario s
$u_{DR,e,up,t,s}$	Shift-up status of electric demand response at time t and scenario s
$u_{DR,e,down,t,s}$	Shift-down status of electric demand response at time t and scenario s
$u_{DR,h,up,t,s}$	Shift-up status of thermal demand response at time t and scenario s
$u_{DR,h,down,t,s}$	Shift-down status of thermal demand response at time t and scenario s
$u_{DR,c,up,t,s}$	Shift-up status of cooling demand response at time t and scenario s
$u_{DR,c,down,t,s}$	Shift-down status of cooling demand response at time t and scenario s
$H_{boil,t,s}$	Heat of boiler at time t and scenario s
$u_{boil,t,s}$	Commitment status of boiler at time t and scenario s
$y_{boil,t,s}$	Boiler's start-up indicator at time t and scenario s
$z_{boil,t,s}$	Boiler's shut-down indicator at time t and scenario s
$C_{AC,t,s}$	Cooling power of absorption chiller at time t and scenario s
$u_{AC,t,s}$	Commitment status of absorption chiller at time t and scenario s
$y_{AC,t,s}$	Absorption chiller's start-up indicator at time t and scenario s
$z_{AC,t,s}$	Absorption chiller's shut-down indicator at time t and scenario s
$H_{EHP,t,s}$	Thermal power of EHP at time t and scenario s
$C_{EHP,t,s}$	Cooling power of EHP at time t and scenario s
$u_{EHP,t,s}$	Commitment status of EHP at time t and scenario s
$y_{EHP,t,s}$	EHP's start-up indicator at time t and scenario s
$z_{EHP,t,s}$	EHP's shut-down indicator at time t and scenario s
$u_{h,EHP,t,s}$	Heating mode indicator of EHP at time t and scenario s
$u_{c,EHP,t,s}$	Cooling mode indicator of EHP at time t and scenario s
$P_{FC,t,s}$	Electric power of FC at time t and scenario s
$H_{FC,t,s}$	Thermal power of FC at time t and scenario s
$u_{FC,t,s}$	Commitment status of FC at time t and scenario s
$y_{FC,t,s}$	Start-up indicator of FC at time t and scenario s
$z_{FC,t,s}$	Shut-down indicator of FC at time t and scenario s
$P_{BSS,ch,t,s}$	Charging power of BSS at time t and scenario s
$P_{BSS,dch,t,s}$	Discharging power of BSS at time t and scenario s
$u_{BSS,ch,t,s}$	Charging status of BSS at time t and scenario s
$u_{BSS,dch,t,s}$	Discharging status of BSS at time t and scenario s
$E_{BSS,t,s}$	State of charge of BSS at time t and scenario s
$E_{BSS,end,s}$	Final state of charge of BSS at scenario s
$H_{TSS,ch,t,s}$	Charging power of TSS at time t and scenario s
$H_{TSS,dch,t,s}$	Discharging power of TSS at time t and scenario s
$u_{TSS,ch,t,s}$	Charging status of TSS at time t and scenario s
$u_{TSS,dch,t,s}$	Discharging status of TSS at time t and scenario s

$E_{TSS,t,s}$	State of charge of TSS at time t and scenario s
$E_{TSS,end,s}$	Final state of charge of TSS at scenario s
$P_{CSS,ch,t,s}$	Charging power of CSS at time t and scenario s
$P_{CSS,dch,t,s}$	Discharging power of CSS at time t and scenario s
$u_{CSS,ch,t,s}$	Charging status of CSS at time t and scenario s
$u_{CSS,dch,t,s}$	Discharging status of CSS at time t and scenario s
$E_{CSS,t,s}$	State of charge of CSS at time t and scenario s
$E_{CSS,end,s}$	Final state of charge of CSS at scenario s
$P_{ev,ch,t,s}$	Charging power of ev th EV at time t and scenario s
$P_{ev,dch,t,s}$	Discharging power of ev th EV at time t and scenario s
$u_{ev,ch,t,s}$	Charging status of ev th EV at time t and scenario s
$u_{ev,dch,t,s}$	Discharging status of ev th EV at time t and scenario s
$E_{ev,t,s}$	State of charge of ev th EV at time t and scenario s
$E_{ev,end,s}$	Final state of charge of ev th EV at scenario s
$DR_{e,up,t,s}$	Shift-up electric demand at time t and scenario s
$DR_{e,down,t,s}$	Shift-down electric demand at time t and scenario s
$DR_{h,up,t,s}$	Shift-up thermal demand at time t and scenario s
$DR_{h,down,t,s}$	Shift-down thermal demand at time t and scenario s
$DR_{c,up,t,s}$	Shift-up cooling demand at time t and scenario s
$DR_{c,down,t,s}$	Shift-down cooling demand at time t and scenario s

1. Introduction

Energy hubs (EHs) are units in which multiple energy carriers are converted, conditioned and stored to simultaneously supply different forms of energy demands such as electric, thermal, cooling, water and hydrogen demands [1, 2]. EH can be considered as a unit with multiple energy carriers as inputs and multiple demands as outputs. The redundant connections between input and output nodes enhances energy supply reliability, energy efficiency and energy security, decreases operation cost and also decreases the sensitivity to energy carriers' price fluctuations. Thanks to their merits, it is expected that in the near future, a large portion of residential/commercial buildings and industrial complexes are operated as EHs. EHs may import power from power grids, natural gas (NG) from NG networks, heat from district heating networks, cooling power from district cooling networks and convert the imported energy carriers with boilers, combined heat and power (CHP) units, fuel cells (FCs) [3-5], electric/absorption chillers and electric heat pumps (EHPs). EHs are commonly equipped with different energy storage systems such as electric storage system (ESS), thermal storage system (TSS), cooling storage system (CSS) or even in some cases power to hydrogen (P2H) and power to gas (P2G) storage systems. Storage systems mitigate the fluctuation of volatile renewable energy resources and enable EH operator to increase the utilisation factor of more efficient units and decrease the utilisation factor of less efficient units; They also enable higher penetration of renewable energy resources. Unit commitment (UC) module in EHs determines day-ahead scheduling of EH components and imported energy carriers in a way that EH operation cost is minimised and all

operational constraints are met. UC in EHs is commonly a mixed-integer linear programming (MILP) problem with a lot of uncertain input data, as the forecasts of demands, renewable generation, etc. are uncertain [6].

In [7], robust optimisation has been used to model the uncertainties of renewable generation in an EH with photovoltaic (PV) module, boiler, CHP unit, absorption chiller, gas turbine, heat recovery unit, EHP, ESS, TSS and P2G. P2G is used to convert the excessive PV power into hydrogen or NG at peak times of PV generation. Electricity and NG are inputs of the EH and electricity, heat and cooling energy are its outputs. Cross demand response (DR) has been used in which consumers may switch between electricity and NG. Dynamic economic load dispatch has been done in which the commitment status of the components is not determined and start-up/shut-down costs are ignored [8]. Degradation of storage systems has not been considered. The results show that similar schedule is found for EH with different uncertainty sets including polyhedral and hybrid box-polyhedral uncertainty sets. The effect of maximum demand response participation factor on EH operation has been investigated.

In [9], information gap decision theory (IGDT) has been used to deal with the uncertainties of UC in an EH with power and NG inputs and heat and power demands. The constraints of power, heat and NG networks have been considered. The degradation and storage loss of storage systems have not been considered and the demands are not responsive. In [10], UC in an EH with boiler, CHP unit, EHP, absorption chiller and battery storage system (BSS) with power, NG, heat and wood chips as inputs and power, heat and cooling demands has been modeled as a MILP model. Storage loss and degradation of the storage system have not been considered and the demands are not responsive. In [11], a risk-averse stochastic method has been used to deal with the uncertainties of demands, wind power, electricity and heat prices in an EH with wind turbine, boiler, CHP unit, ESS, TSS, responsive electric and thermal demands. Due to the existence of heat market, the heat prices have been assumed uncertain. Downside risk is calculated and bounded for each scenario. Power, NG and heat are the inputs of the hub and electric, heat and NG demands are its outputs.

In [12], risk-averse information gap decision theory (IGDT) has been used to deal with the uncertainties of electricity and heat demands and wind power in an EH with boiler, wind turbine, CHP and fleet of electric vehicles (EVs), power and NG inputs, non-responsive electricity and heat demands. The degradation costs and storage loss of EV batteries have been ignored. In [13], Monte Carlo Simulation (MCS) has been used to model the uncertainties of demands, heat and electricity market prices and wind speed in an EH with boiler, wind turbine, ESS and TSS, power, heat and NG inputs, electricity, heat and NG demands, while electric and heat demands are responsive; start-up and shut-down costs of EH components have been ignored. In [14], robust optimisation has been used to deal with the uncertainties of electricity prices in an EH with power, NG and hydrogen as inputs and power, heat, hydrogen and NG as outputs. The EH includes gas turbine, FC, CHP, boiler, wind turbine, ESS,

TSS, gas storage and hydrogen storage systems. The electric and thermal demands have been assumed responsive. The export of hydrogen has been used to decrease EH operation cost. Degradation and storage loss of storage systems have not been considered.

In [15], robust optimisation has been used to deal with the uncertainties in UC for an EH with gas turbine, heat recovery unit, boiler, electric and absorption chillers, BSS, TSS, CSS, PV and wind turbine (WT) wherein the inputs are power and NG and outputs are responsive electricity, heat and cooling demands. Degradation and storage loss of storage systems have not been considered. In [16], the scheduling of a residential EH with power generation unit, heat recovery unit, boiler, electric and absorption chillers, PV, TSS, plug-in hybrid EVs, TSS, curtailable and shiftable home appliances, power and NG inputs and electricity, heat and cooling demands has been done. The comfort of consumers in terms of temperature level and waiting time as well as emissions have been considered and UC has been formulated as a multi-objective optimisation problem which is solved by epsilon constraint method; however, the uncertainties have not been considered and degradation and storage loss of storage systems have been ignored. In [17], MCS and interval optimisation have been used to deal with uncertainties of an EH with WT, boiler, CHP, ESS and TSS having NG, heat and power as inputs and NG, heat and power as demands. The uncertainties of demands have been modeled with MCS and interval optimisation has been used to deal with the uncertainties of electricity prices.

Regarding the reviewed literature in UC for EH, the following points must be highlighted.

- In some cases, the uncertainties of demands and renewable generation have not been considered.
- The effect of intelligent EV parking lots on operation of EH has not been investigated.
- In most of the cases, the degradation of storage systems and their storage loss have not been considered.
- The optimal commitment of cooling components has not been determined in EH operation.

In this research, the objective is to develop a new stochastic model for UC in EHs including intelligent EV parking lot, boiler, PV module, FC, absorption chiller, EHP, with electricity and NG as inputs and electricity, heat, cooling and NG demands, considering the uncertainties of demands, PV power and initial energy level of EV's batteries. The contributions of this research are as follows:

- ✓ The uncertainties of electricity, heat, cooling and NG demands, PV power as well as the uncertainties of initial energy level of EV batteries have been considered and modelled with MCS.

- ✓ Responsive electric, thermal and cooling demands have been used and the effect of demand response on EH operation has been investigated.
- ✓ Comprehensive models for storage systems and EV's batteries have been used considering their degradation and storage loss.
- ✓ An intelligent parking lot has been integrated into EH and the effect of EV fleet with vehicle to grid (V2G) capability on EH operation has been investigated.
- ✓ Optimal commitment of cooling components has been determined considering their ramp-up/down rate limits and start-up/shut-down costs.

2. Methods and materials

The proposed stochastic model for UC in EH is represented by (1)-(90). The expected operation cost of EH, given by (1), is minimised as the objective. The operation cost of EH in each scenario is characterised by (2)-(10). As per (2), EH operation cost includes the cost of purchased electricity and NG, start-up and shut-down cost of components, load shed costs, degradation cost of BSS, TSS, CSS and EV batteries as well as the incentives paid to responsive consumers. As per (3)-(6), the degradation cost of storage systems is proportional to their replacement cost, proportional to sum of their charging and discharging power and inversely proportional to their total charge-discharge capacity. Equations (7) represent the total incentive paid to demands and (8)-(10) respectively represent the incentives paid to electric, thermal and cooling demands.

$$\overline{OC} = \sum_s pr_s OC_s \quad (1)$$

$$\begin{aligned} OC_s = & \sum_t \pi_{grid,t} \cdot P_{grid,t,s} + \sum_t \pi_{NG,t} \cdot P_{NG,t,s} + \sum_t (y_{boil,t,s} \cdot SU_{boil} + z_{boil,t,s} \cdot SD_{boil}) + \sum_t (y_{FC,t,s} \cdot SU_{FC} + z_{FC,t,s} \cdot SD_{FC}) \\ & + \sum_t (y_{EHP,t,s} \cdot SU_{EHP} + z_{EHP,t,s} \cdot SD_{EHP}) + \sum_t (y_{AC,t,s} \cdot SU_{AC} + z_{AC,t,s} \cdot SD_{AC}) \\ & + \sum_t (VLL_e \cdot P_{shed,t,s} + VLL_h \cdot H_{shed,t,s} + VLL_c \cdot C_{shed,t,s}) + d_{BSS,s} + d_{TSS,s} + d_{CSS,s} + d_{fleet,s} + DRC_s \quad \forall s \quad (2) \end{aligned}$$

$$d_{BSS,s} = \frac{RC_{BSS}}{TCDC_{BSS}} \sum_t (P_{BSS,ch,t,s} + P_{BSS,dch,t,s}) \quad \forall s \quad (3)$$

$$d_{TSS,s} = \frac{RC_{TSS}}{TCDC_{TSS}} \sum_t (P_{TSS,ch,t,s} + P_{TSS,dch,t,s}) \quad \forall s \quad (4)$$

$$d_{CSS,s} = \frac{RC_{CSS}}{TCDC_{CSS}} \sum_t (P_{CSS,ch,t,s} + P_{CSS,dch,t,s}) \quad \forall s \quad (5)$$

$$d_{fleet,s} = \sum_{ev} \left(\frac{RC_{ev}}{TCDC_{ev}} \sum_t (P_{ev,ch,t,s} + P_{ev,dch,t,s}) \right) \quad \forall s \quad (6)$$

$$DRC_s = DRC_{e,s} + DRC_{h,s} + DRC_{c,s} \quad \forall s \quad (7)$$

$$DRC_{e,s} = \sum_t DRI_e (DR_{e,up,t,s} + DR_{e,down,t,s}) \quad \forall s \quad (8)$$

$$DRC_{h,s} = \sum_t DRI_h (DR_{h,up,t,s} + DR_{h,down,t,s}) \quad \forall s \quad (9)$$

$$DRC_{c,s} = \sum_t DRI_c (DR_{c,up,t,s} + DR_{c,down,t,s}) \quad \forall s \quad (10)$$

The sufficiency of supply of electricity, heat, cooling power and NG can be respectively represented by (11)-(14). As per (11), for each scenario at each time, sum of electric power generated by FC, power injected by PV, power imported from grid, electric load shed, discharging power of BSS and EVs and shift-down electric demand should not be less than sum of electric demand, charging power of BSS, CSS and EVs, shift-up electric demand and electric power fed into EHP. As per (12), for each scenario and at each time, sum of thermal power generated by FC, boiler and EHP, thermal load shed, discharging power of TSS and shift-down thermal demand should not be less than sum of thermal demand, charging power of TSS, shift-up thermal demand and thermal power fed into absorption chiller. As per (13), for each scenario and at each time, sum of cooling power generated by absorption chiller and EHP, cooling load shed, discharging power of CSS and shift-down cooling demand should not be less than sum of cooling demand and shift-up cooling demand. As per (14), for each scenario and at each time, the NG imported from NG network must be equal to the NG fed into FC and boiler plus NG demand.

$$P_{grid,t} eff_{TF} + P_{FC,t,s} + eff_{conv} PV_{t,s} + P_{shed,t,s} + P_{BSS,dch,t,s} + DR_{e,down,t,s} + \sum_{ev} P_{ev,dch,t,s} \\ \geq D_{e,t,s} + DR_{e,up,t,s} + P_{BSS,ch,t,s} + \sum_{ev} P_{ev,ch,t,s} + P_{CSS,ch,t,s} + \frac{H_{EHP,t,s}}{COP_{EHP,h}} + \frac{C_{EHP,t,s}}{COP_{EHP,c}} \quad \forall t, \forall s \quad (11)$$

$$H_{boil,t,s} + H_{FC,t,s} + H_{shed,t,s} + H_{TSS,dch,t,s} + H_{EHP,t,s} + DR_{h,down,t,s} \geq D_{h,t,s} + DR_{h,up,t,s} + H_{TSS,ch,t,s} + \frac{C_{AC,t,s}}{COP_{AC}} \quad \forall t, \forall s \quad (12)$$

$$C_{AC,t,s} + C_{shed,t,s} + C_{CSS,dch,t,s} + C_{EHP,t,s} + DR_{c,down,t,s} \geq D_{c,t,s} + DR_{c,up,t,s} \quad \forall t, \forall s \quad (13)$$

$$P_{NG,t,s} = \frac{P_{FC,t,s}}{eff_{P,FC}} + \frac{H_{boil,t,s}}{eff_{boil}} + D_{NG,t,s} \quad \forall t, \forall s \quad (14)$$

The shift-up and shift-down of responsive electric demands is constrained by (15)-(18) [11]. As per (15), at each time and each scenario, the shift-up electric demand is bounded by the shift-up electric demand participation factor times the electric demand; similarly (16) indicates that at each time and each scenario, the shift-down electric demand is bounded by the shift-down electric demand participation factor times the electric demand. Constraints (17) ensure that at each time and scenario, electric demand cannot be simultaneously shifted up and shifted down. Constraints (18) ensure that at each scenario, the summation of shift-up electric demands over operation horizon equals the summation of shift-down electric demands over operation horizon.

$$DR_{e,up,t,s} \leq DPF_{e,up} \cdot D_{e,t,s} \cdot u_{DR,e,up,t,s} \quad \forall t, \forall s \quad (15)$$

$$DR_{e,down,t,s} \leq DPF_{e,down} \cdot D_{e,t,s} \cdot u_{DR,e,down,t,s} \quad \forall t, \forall s \quad (16)$$

$$u_{DR,e,up,t,s} + u_{DR,e,down,t,s} \leq 1 \quad \forall t, \forall s \quad (17)$$

$$\sum_t DR_{e,up,t,s} = \sum_t DR_{e,down,t,s} \quad \forall s \quad (18)$$

The shift-up and shift-down of responsive thermal demands is constrained by (19)-(22) [11]. As per (19), at each time and each scenario, the shift-up thermal demand is bounded by the shift-up thermal demand participation factor times the thermal demand; similarly (20) indicates that at each time and each scenario, the shift-down thermal demand is bounded by the shift-down thermal demand participation factor times the thermal demand. Constraints (21) ensure that at each time and scenario, thermal demand cannot be simultaneously shifted up and shifted down. Constraints (22) ensure that at each scenario, the summation of shift-up thermal demands must be equal to the summation of shift-down thermal demands.

$$DR_{h,up,t,s} \leq DPF_{h,up} \cdot D_{h,t,s} \cdot u_{DR,h,up,t,s} \quad \forall t, \forall s \quad (19)$$

$$DR_{h,down,t,s} \leq DPF_{h,down} \cdot D_{h,t,s} \cdot u_{DR,h,down,t,s} \quad \forall t, \forall s \quad (20)$$

$$u_{DR,h,up,t,s} + u_{DR,h,down,t,s} \leq 1 \quad \forall t, \forall s \quad (21)$$

$$\sum_t DR_{h,up,t,s} = \sum_t DR_{h,down,t,s} \quad \forall s \quad (22)$$

The shift-up and shift-down of responsive cooling demands is constrained by (23)-(26) [11]. As per (23), at each time and each scenario, the shift-up cooling demand is bounded by the shift-up cooling demand participation factor times the cooling demand; similarly (24) signifies that at each time and each scenario, the shift-down cooling demand is bounded by the shift-down cooling demand participation factor times the cooling demand. Constraints (25) make sure that at each time and each scenario, cooling demand cannot be simultaneously shifted up and shifted down. Constraints (26) ensure that at each scenario, the summation of shift-up cooling demands over operation horizon equals the summation of shift-down cooling demands over operation horizon.

$$DR_{c,up,t,s} \leq DPF_{c,up} \cdot D_{c,t,s} \cdot u_{DR,c,up,t,s} \quad \forall t, \forall s \quad (23)$$

$$DR_{c,down,t,s} \leq DPF_{c,down} \cdot D_{c,t,s} \cdot u_{DR,c,down,t,s} \quad \forall t, \forall s \quad (24)$$

$$u_{DR,c,up,t,s} + u_{DR,c,down,t,s} \leq 1 \quad \forall t, \forall s \quad (25)$$

$$\sum_t DR_{c,up,t,s} = \sum_t DR_{c,down,t,s} \quad \forall s \quad (26)$$

The operation of the boiler is subject to the constraints (27)-(33). The boiler and all other EH components have been assumed ON at the beginning of the operation horizon. Constraints (27)-(30) define start-up and shut-down indicators of boiler, i.e., $y_{boil,t,s}$ and $z_{boil,t,s}$. Constraints (31) ensure that at each time and scenario the heat of committed boiler is bounded to a pre-specified allowable range. Constraints (32) ensure that at each time and scenario, the thermal power increase of boiler does not exceed its ramp-up rate limit; eventually constraints (33) ensure that the thermal power reduction of boiler does not exceed its ramp-down rate limit.

$$y_{boil,t,s} - z_{boil,t,s} = u_{boil,t,s} - u_{boil,t-1,s} \quad \forall s, \forall t \neq 1 \quad (27)$$

$$y_{boil,t,s} = 0 \quad \forall s, \forall t = 1 \quad (28)$$

$$z_{boil,t,s} = 1 - u_{boil,t,s} \quad \forall s, \forall t = 1 \quad (29)$$

$$y_{boil,t,s} + z_{boil,t,s} \leq 1 \quad \forall s, \forall t \quad (30)$$

$$H_{boil,min} u_{boil,t,s} \leq H_{boil,t,s} \leq H_{boil,max} u_{boil,t,s} \quad \forall s, \forall t \quad (31)$$

$$H_{boil,t+1,s} - H_{boil,t,s} \leq RU_{boil} \quad \forall s, \forall t \neq 24 \quad (32)$$

$$H_{boil,t-1,s} - H_{boil,t,s} \leq RD_{boil} \quad \forall s, \forall t \neq 1 \quad (33)$$

The operation of the FC is subject to the constraints (34)-(43). Constraints (34)-(37) define start-up and shut-down indicators of FC, i.e., $y_{FC,t,s}$ and $z_{FC,t,s}$. Constraints (38) and (39) respectively ensure that the power and heat of committed FC is confined within their pre-specified allowable ranges. Constraints (40) ensure that the electric power increase of FC does not violate its power ramp-up rate limit and constraints (41) ensure that its

electric power decrease does not exceed its power ramp-down rate limit. Constraints (42) ensure that the thermal power increase of FC does not exceed its heat ramp-up rate limit and constraints (43) ensure that the thermal power decrease of FC does not exceed its heat ramp-down rate limit.

$$y_{FC,t,s} - z_{FC,t,s} = u_{FC,t,s} - u_{FC,t-1,s} \quad \forall s, \forall t \neq 1 \quad (34)$$

$$y_{FC,t,s} = 0 \quad \forall s, \forall t = 1 \quad (35)$$

$$z_{FC,t,s} = 1 - u_{FC,t,s} \quad \forall s, \forall t = 1 \quad (36)$$

$$y_{FC,t,s} + z_{FC,t,s} \leq 1 \quad \forall s, \quad \forall t \quad (37)$$

$$P_{FC,min} u_{FC,t,s} \leq P_{FC,t,s} \leq P_{FC,max} u_{FC,t,s} \quad \forall s, \quad \forall t \quad (38)$$

$$H_{FC,min} u_{FC,t,s} \leq H_{FC,t,s} \leq H_{FC,max} u_{FC,t,s} \quad \forall s, \quad \forall t \quad (39)$$

$$P_{FC,t+1,s} - P_{FC,t,s} \leq RU_{P,FC} \quad \forall s, \forall t \neq 24 \quad (40)$$

$$P_{FC,t-1,s} - P_{FC,t,s} \leq RD_{P,FC} \quad \forall s, \forall t \neq 1 \quad (41)$$

$$H_{FC,t+1,s} - H_{FC,t,s} \leq RU_{H,FC} \quad \forall s, \forall t \neq 24 \quad (42)$$

$$H_{FC,t-1,s} - H_{FC,t,s} \leq RD_{H,FC} \quad \forall s, \forall t \neq 1 \quad (43)$$

The operation of the EHP is subject to the constraints (44)-(54). As per (44), the committed EHP is either in heating mode or in cooling mode. Constraints (45)-(48) define start-up and shut-down indicators of EHP. Constraints (49) ensure that in heating mode the thermal power of committed EHP is confined within its pre-specified allowable range. Constraints (50) ensure that the thermal power increase of EHP does not violate its thermal power ramp-up rate limit and constraints (51) ensure that the thermal power decrease of EHP does not exceed its thermal power ramp-down rate limit. Constraints (52) ensure that in cooling mode the cooling power of committed EHP is confined within its pre-specified allowable range. Constraints (53) ensure that the cooling power increase of EHP does not violate its cooling power ramp-up rate limit and constraints (54) ensure that the cooling power decrease of EHP does not exceed its cooling power ramp-down rate limit.

$$u_{h,EHP,t,s} + u_{c,EHP,t,s} = u_{EHP,t,s} \quad \forall s, \forall t \quad (44)$$

$$y_{EHP,t,s} - z_{EHP,t,s} = u_{EHP,t,s} - u_{EHP,t-1,s} \quad \forall s, \quad \forall t \neq 1 \quad (45)$$

$$y_{EHP,t,s} = 0 \quad \forall s, \forall t = 1 \quad (46)$$

$$z_{EHP,t,s} = 1 - u_{EHP,t,s} \quad \forall s, \quad \forall t = 1 \quad (47)$$

$$y_{EHP,t,s} + z_{EHP,t,s} \leq 1 \quad \forall s, \quad \forall t \quad (48)$$

$$H_{EHP,min} u_{h,EHP,t,s} \leq H_{EHP,t,s} \leq H_{EHP,max} u_{h,EHP,t,s} \quad \forall s, \forall t \quad (49)$$

$$H_{EHP,t+1,s} - H_{EHP,t,s} \leq RU_{EHP,h} \quad \forall s, \quad \forall t \neq 24 \quad (50)$$

$$H_{EHP,t-1,s} - H_{EHP,t,s} \leq RD_{EHP,h} \quad \forall s, \quad \forall t \neq 1 \quad (51)$$

$$C_{EHP,min}u_{c,EHP,t,s} \leq C_{EHP,t,s} \leq C_{EHP,max} u_{c,EHP,t,s} \quad \forall s, \forall t \quad (52)$$

$$C_{EHP,t+1,s} - C_{EHP,t,s} \leq RU_{EHP,c} \quad \forall s, \forall t \neq 24 \quad (53)$$

$$C_{EHP,t-1,s} - C_{EHP,t,s} \leq RD_{EHP,c} \quad \forall s, \forall t \neq 1 \quad (54)$$

The operation of the absorption chiller is constrained by (55)-(61). Constraints (55)-(58) define start-up and shut-down indicators of absorption chiller. Constraints (59) ensure that the cooling power of the committed absorption chiller is confined within its pre-specified range. Constraints (60) ensure that the cooling power increase of absorption chiller does not exceed its ramp-up rate limit and constraints (61) ensure that the cooling power decrease of absorption chiller does not violate its ramp-down rate limit.

$$y_{AC,t,s} - z_{AC,t,s} = u_{AC,t,s} - u_{AC,t-1,s} \quad \forall s, \forall t \neq 1 \quad (55)$$

$$y_{AC,t,s} = 0 \quad \forall s, \forall t = 1 \quad (56)$$

$$z_{AC,t,s} = 1 - u_{AC,t,s} \quad \forall s, \forall t = 1 \quad (57)$$

$$y_{AC,t,s} + z_{AC,t,s} \leq 1 \quad \forall s, \forall t \quad (58)$$

$$C_{AC,min}u_{AC,t,s} \leq C_{AC,t,s} \leq C_{AC,max} u_{AC,t,s} \quad \forall s, \forall t \quad (59)$$

$$C_{AC,t+1,s} - C_{AC,t,s} \leq RU_{AC} \quad \forall s, \forall t \neq 24 \quad (60)$$

$$C_{AC,t-1,s} - C_{AC,t,s} \leq RD_{AC} \quad \forall s, \forall t \neq 1 \quad (61)$$

The operation of EV batteries is subject to the constraints (62)-(69). According to (62) and (63), charging and discharging power of EV batteries must be confined within their pre-specified intervals. According to (64), the energy level of each EV battery at each time and scenario should not fall below a minimum limit and go beyond an upper limit. Constraints (65) ensure that batteries cannot be simultaneously charged and discharged. Constraints (66) ensure that the final energy level of each EV battery is equal to its initial energy level. As per (67)-(68), the energy level of each EV battery at each time is equal to sum of its energy level at previous time and the energy added during charging process minus the sum of storage loss and the discharging energy that is absorbed from it. As (69), when EVs are not in the parking lot, batteries are in idle mode, as UTS_{ev} represents the set of times that ev th EV is not available in the parking lot.

$$u_{ev,ch,t,s}P_{ch_{ev,min}} \leq P_{ev,ch,t,s} \leq u_{ev,ch,t,s}P_{ch_{ev,max}} \quad \forall s, \forall ev, \forall t \quad (62)$$

$$u_{ev,dch,t,s}P_{dch_{ev,min}} \leq P_{ev,dch,t,s} \leq u_{ev,dch,t,s}P_{dch_{ev,max}} \quad \forall s, \forall ev, \forall t \quad (63)$$

$$E_{ev,min} \leq E_{ev,t,s} \leq E_{ev,max} \quad \forall s, \forall ev, \forall t \quad (64)$$

$$u_{ev,ch,t,s} + u_{ev,dch,t,s} \leq 1 \quad \forall s, \forall ev, \forall t \quad (65)$$

$$E_{ev,ini} = E_{ev,end,s} \quad \forall s, \forall ev \quad (66)$$

$$E_{ev,t,s} = E_{ev,t-1,s} - \frac{P_{ev,dch,t,s}}{eff_{ev,dch}} + eff_{ev,ch}P_{ev,ch,t,s} - SLF_{ev} \left(\frac{E_{ev,t,s} + E_{ev,t-1,s}}{2} \right) \quad \forall s, \forall ev, \forall t \neq 1 \quad (67)$$

$$E_{ev,t,s} = E_{ev,ini,s} - \frac{P_{ev,dch,t,s}}{eff_{ev,dch}} + eff_{ev,ch}P_{ev,ch,t,s} - SLF_{ev} \left(\frac{E_{ev,t,s} + E_{ev,t-1,s}}{2} \right) \quad \forall s, \forall ev, \forall t = 1 \quad (68)$$

$$u_{ev,ch,t,s} + u_{ev,dch,t,s} = 0 \quad \forall s, \forall ev, \forall t \in UTS_{ev} \quad (69)$$

The operation of BSS is subject to the constraints (70)-(76). According to (70) and (71), charging and discharging power of BSS must be confined within their pre-specified intervals. According to (72), the energy level of BSS at each time and scenario should not be less than a minimum limit and higher than a maximum limit. Constraints (73) ensure that BSS cannot experience simultaneous charging and discharging. Constraints (74) guarantee that the energy level of BSS at the end of operation horizon is equal to its initial energy level. As per (75)-(76), the energy level of BSS at each time is equal to sum of its energy level at previous time and the energy added during charging process minus the sum of storage loss and the discharging energy that is reduced from BSS. Similar to BSS, the constraints of TSS and CSS can be respectively represented as (77)-(83) and (84)-(90).

$$u_{BSS,ch,t,s}Pch_{BSS,min} \leq P_{BSS,ch,t,s} \leq u_{BSS,ch,t,s}Pch_{BSS,max} \quad \forall s, \forall t \quad (70)$$

$$u_{BSS,dch,t,s}Pdch_{BSS,min} \leq P_{BSS,dch,t,s} \leq u_{BSS,dch,t,s}Pdch_{BSS,max} \quad \forall s, \forall t \quad (71)$$

$$E_{BSS,min} \leq E_{BSS,t,s} \leq E_{BSS,max} \quad \forall s, \forall t \quad (72)$$

$$u_{BSS,ch,t,s} + u_{BSS,dch,t,s} \leq 1 \quad \forall s, \forall t \quad (73)$$

$$E_{BSS,ini} = E_{BSS,end,s} \quad \forall s \quad (74)$$

$$E_{BSS,t,s} = E_{BSS,t-1,s} - \frac{P_{BSS,dch,t,s}}{eff_{BSS,dch}} + eff_{BSS,ch}P_{BSS,ch,t,s} - SLF_{BSS} \left(\frac{E_{BSS,t,s} + E_{BSS,t-1,s}}{2} \right) \quad \forall s, \forall t \neq 1 \quad (75)$$

$$E_{BSS,t,s} = E_{BSS,ini} - \frac{P_{BSS,dch,t,s}}{eff_{BSS,dch}} + eff_{BSS,ch}P_{BSS,ch,t,s} - SLF_{BSS} \left(\frac{E_{BSS,t,s} + E_{BSS,t-1,s}}{2} \right) \quad \forall s, \forall t = 1 \quad (76)$$

$$u_{TSS,ch,t,s}Hch_{TSS,min} \leq H_{TSS,ch,t,s} \leq u_{TSS,ch,t,s}Hch_{TSS,max} \quad \forall s, \forall t \quad (77)$$

$$u_{TSS,dch,t,s}Hdch_{TSS,min} \leq H_{TSS,dch,t,s} \leq u_{TSS,dch,t,s}Hdch_{TSS,max} \quad \forall s, \forall t \quad (78)$$

$$E_{TSS,min} \leq E_{TSS,t,s} \leq E_{TSS,max} \quad \forall s, \forall t \quad (79)$$

$$u_{TSS,ch,t,s} + u_{TSS,dch,t,s} \leq 1 \quad \forall s, \forall t \quad (80)$$

$$E_{TSS,ini} = E_{TSS,end,s} \quad \forall s \quad (81)$$

$$E_{TSS,t,s} = E_{TSS,t-1,s} - \frac{H_{TSS,dch,t,s}}{eff_{TSS,dch}} + eff_{TSS,ch}H_{TSS,ch,t,s} - SLF_{TSS} \left(\frac{E_{TSS,t,s} + E_{TSS,t-1,s}}{2} \right) \quad \forall s, \forall t \neq 1 \quad (82)$$

$$E_{TSS,t,s} = E_{TSS,ini} - \frac{H_{TSS,dch,t,s}}{eff_{TSS,dch}} + eff_{TSS,ch}H_{TSS,ch,t,s} - SLF_{TSS} \left(\frac{E_{TSS,t,s} + E_{TSS,t-1,s}}{2} \right) \quad \forall s, \forall t = 1 \quad (83)$$

$$u_{CSS,ch,t,s}Pch_{CSS,min} \leq P_{CSS,ch,t,s} \leq u_{CSS,ch,t,s}Pch_{CSS,max} \quad \forall s, \forall t \quad (84)$$

$$u_{CSS,dch,t,s}Pdch_{CSS,min} \leq P_{CSS,dch,t,s} \leq u_{CSS,dch,t,s}Pdch_{CSS,max} \quad \forall s, \forall t \quad (85)$$

$$u_{CSS,ch,t,s} + u_{CSS,dch,t,s} \leq 1 \quad \forall s, \forall t \quad (86)$$

$$E_{CSS,ini} = E_{CSS,end,s} \quad \forall s \quad (87)$$

$$E_{CSS,t,s} = E_{CSS,t-1,s} - \frac{P_{CSS,dch,t,s}}{eff_{CSS,dch}} + COP_{CSS}P_{CSS,ch,t,s} - SLF_{CSS} \left(\frac{E_{CSS,t,s} + E_{CSS,t-1,s}}{2} \right) \quad \forall s, \forall t \neq 1 \quad (88)$$

$$E_{CSS,t,s} = E_{CSS,ini} - \frac{P_{CSS,dch,t,s}}{eff_{CSS,dch}} + COP_{CSS}P_{CSS,ch,t,s} - SLF_{CSS} \left(\frac{E_{CSS,t,s} + E_{CSS,t-1,s}}{2} \right) \quad \forall s, \forall t = 1 \quad (89)$$

$$E_{CSS,min} \leq E_{CSS,t,s} \leq E_{CSS,max} \quad \forall s, \forall t \quad (90)$$

3. Results and discussion

An EH with boiler, FC, CHP, EHP, absorption chiller, transformer, PV module and its converter, BSS, TSS, CSS and a parking lot with 12 EVs has been used as case study. The power and NG are imported from power grid and NG network and electric, thermal, cooling and NG demands are supplied by EH. The scheme of the studied EH

can be seen as Fig.1. Electric, thermal and cooling demands are responsive and a portion of demands may be shed if needed. EH purchases power with a time of use (TOU) tariff and purchases NG from NG network with a fixed tariff. Table 1 includes time factors of demands and PV power, Table 2 contains data of storage systems and Table 3 includes other input data of EH. In this paper, the default units for time, power and cost are hour (h), kW and US \$. The operation horizon is one day and operation resolution is 1 hour. The proposed MILP model for UC in EH is solved with CPLEX solver in general algebraic modeling system (GAMS) which guarantees the achievement of the global minimum. In 3.1, the model is solved ignoring the uncertainties; in 3.2, the uncertainties of demands, PV power and EV batteries are considered and the resulted stochastic model is solved. In 3.3, the effect of parking lot and EV fleet on EH operation is investigated; finally in 3.4, the effects of electric, thermal and cooling demand response on EH operation are investigated in details.

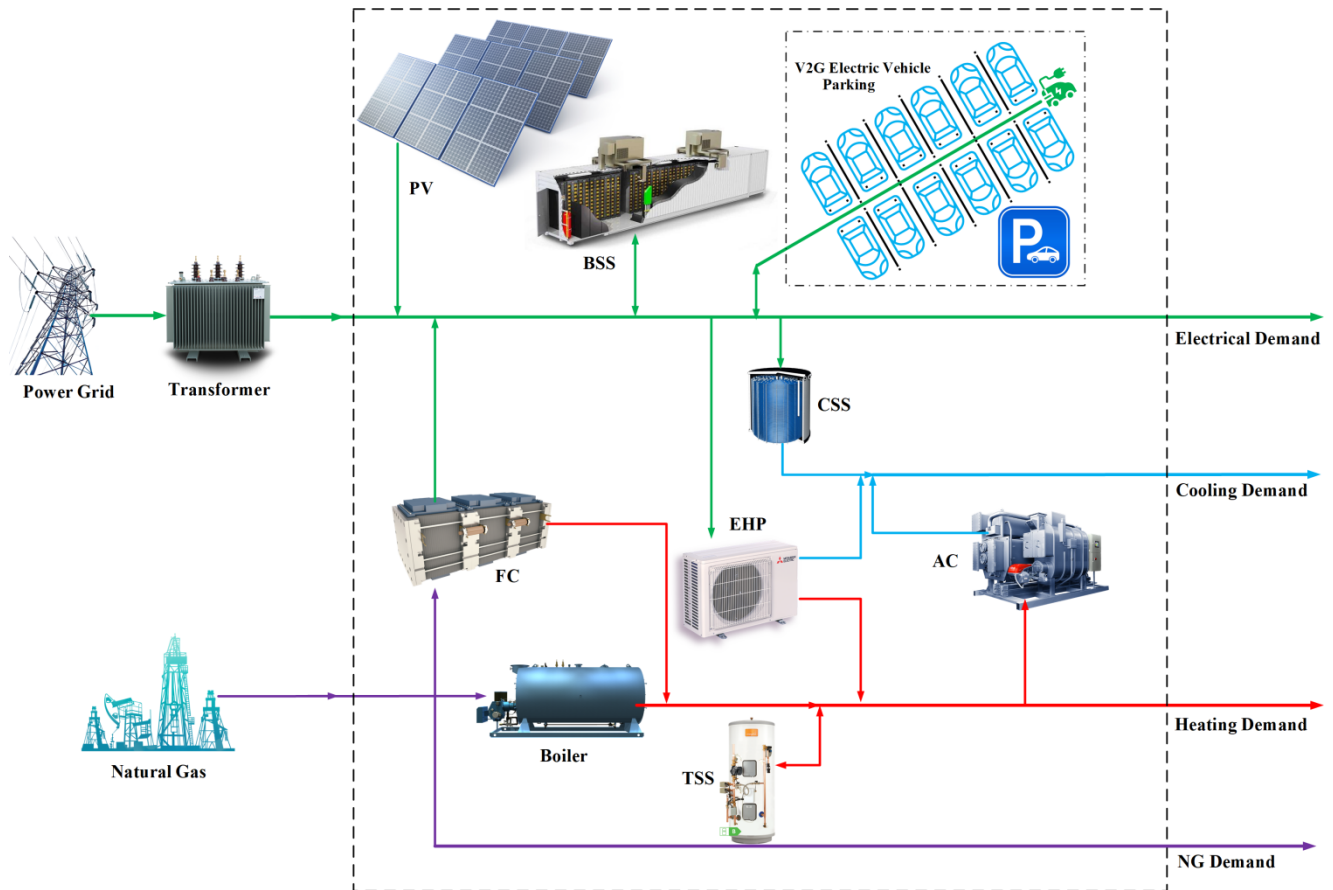


Fig.1. Architecture of the studied EH

Table 1. Time factors of demands and PV power [18]

Hour	Electric demand	Thermal demand	Cooling demand	NG demand	PV power [19]	Hour	Electric demand	Thermal demand	Cooling demand	NG demand	PV power [19]
1	0.3934	0.3282	0.2668	0.2425	0	13	0.9281	0.9467	1.0000	0.9750	1.0000
2	0.3923	0.3181	0.2496	0.2375	0	14	0.9435	0.9660	0.9899	0.9500	0.9040
3	0.3772	0.2722	0.2341	0.2325	0	15	0.9570	1.0000	0.9610	0.6250	0.8105
4	0.3732	0.2534	0.2319	0.3000	0	16	0.9607	0.9385	0.9082	0.5100	0.6980
5	0.4397	0.3470	0.2523	0.3125	0.02	17	0.9661	0.9481	0.8005	0.5275	0.4675
6	0.5753	0.4998	0.3385	0.4625	0.1080	18	1.0000	0.8794	0.7358	0.4875	0.2520
7	0.6922	0.5505	0.4643	0.4775	0.2790	19	0.9987	0.8969	0.6566	0.8250	0.0940
8	0.8378	0.6888	0.6581	0.6325	0.5190	20	0.9594	0.8340	0.5775	0.9750	0.0200
9	0.8814	0.7634	0.8117	0.5950	0.7424	21	0.8603	0.8134	0.5160	1.0000	0.0010
10	0.8953	0.8873	0.9238	0.6125	0.9184	22	0.7153	0.6809	0.4422	0.7775	0
11	0.8933	0.9407	1.0000	0.6875	0.9755	23	0.5697	0.4883	0.3475	0.5275	0
12	0.9128	0.9811	0.9954	1.0000	0.9678	24	0.4057	0.4189	0.2569	0.3300	0

Table 2. Data of storage systems and EV batteries

Storage system	Minimum charging power	Maximum charging power	Minimum discharging power	Maximum discharging power	Charging efficiency	Discharging efficiency	Minimum energy	Maximum energy	initial energy	Storage loss factor	Replacement cost	Charge-discharge capacity
ESS	10	40	10	40	0.95	0.95	20	150	20	0.01	20000	4e6
TSS	10	40	10	40	0.9	0.9	20	150	20	0.01	5000	4e6
CSS	10	30	10	30	2	0.95	20	100	20	0.01	5000	4e6
EV batteries	10	40	10	40	0.95	0.95	15	75	20	0.01	20000	4e6

Table 3. Other input data of EH operation problem

Maximum purchasable electricity from grid	400kW	Thermal ramp down of FC	200 kW/h
Maximum purchasable NG	600 kW	Number of EVs	12
Peak electric demand	720 kW	Unavailability time of EVs in parking lot	8-15
Peak thermal demand	350 kW	TOU peak price factor	1
Peak cooling demand	150 kW	TOU mid-peak price factor	0.6
Peak NG demand	180 kW	TOU off-peak price factor	0.3
PV capacity	400 kW	Peak hours of electricity tariff	12-14, 19-22
Power range of FC	60-300 kW	Mid-peak hours of electricity tariff	9-11, 15-18
Heat range of FC	40-200 kW	Off-Peak hours of electricity tariff	23-8
Heat range of boiler	50-220 kW	FC power efficiency	0.45
Heat range of EHP	20-110 kW	FC thermal efficiency	0.3
Cooling power range of EHP	20-110 kW	Boiler efficiency	0.85
Cooling power range of chiller	20-45 kW	EHP thermal COP	3.5
Start up cost of FC	\$10	EHP cooling COP	3.5
Start up cost of boiler	\$10	COP of absorption chiller	0.75
Start up cost of EHP	\$4	Electric DR incentive	1 Cents/kWh
Start up cost of chiller	\$3	Thermal DR incentive	0.5 Cents/kWh
Shut down cost of FC	\$10	Cooling DR incentive	0.3 Cents/kWh
Shut down cost of boiler	\$10	Participation factor for electric, thermal and cooling DR	0.2
Shut down cost of EHP	\$4	Value of lost electric load	1 \$/kWh
Shut down cost of chiller	\$4	Value of lost thermal load	0.5 \$/kWh
Power ramp up of FC	50 kW/h	Value of lost cooling load	0.5 \$/kWh
thermal ramp up of FC	40 kW/h	Transformer efficiency	0.95
Ramp up of boiler	50 kW/h	PV converter efficiency	0.95
Ramp up of chiller	30 kW/h	Peak electricity price	10 Cents/kWh
Cooling ramp up of EHP	40 kW/h	NG price	3 Cents/kWh
Power ramp down of FC	300 kW/h	Scheduling horizon	1 hour
Ramp down of boiler	220 kW/h	Cooling ramp down of EHP	110 kW/h
Ramp down of chiller	45 kW/h	Heat ramp up of EHP	110 kW/h
Heat ramp down of EHP	110 kW/h		

3.1. EH scheduling without uncertainties

In this subsection, UC in the EH is solved ignoring all the uncertainties. According to the results achieved by CPLEX solver, EH operation cost is \$896.5105 and the share of different components in EH operation cost can be seen as Table 4. The imported energy carriers, schedule of electric, thermal and cooling power resources can be respectively seen as Figs. 2-5. No shed for electric and thermal loads is required; as per optimal schedule, only shed of cooling load at hours 10 and 21 respectively with 0.856 kW and 1.92 kW is needed. The charging and discharging power of electric, thermal and cooling storage systems can be seen as Figs. 6-8 and Table 5 includes operation mode and charging/discharging power of EVs. Shift-up/down electric, thermal and cooling demands have been illustrated as Figs. 9-11. According to Table 4, the cost of purchased electricity and NG constitute 95% of EH operation cost. The cost of purchased electricity and NG respectively constitute 51.45% and 43.6% of EH operation cost; 3% of EH operation cost is the incentives paid to responsive electric, thermal and cooling demands.

Table 4. Components of EH operation cost

EH operation cost	\$896.5105	CSS degradation cost	\$0.4678
Cost of purchased electricity	\$461.2809	Total storage degradation cost	\$2.6411
Cost of purchased NG cost	\$390.9941	EV batteries degradation cost	\$6.205
Total load shed cost	\$1.388	Electric DR cost	\$22.2475
Total start up/shut down cost	\$7.0000	Thermal DR cost	\$3.6273
ESS degradation cost	\$1.8470	Cooling DR cost	\$1.1266
TSS degradation cost	\$0.3263	Total DR cost	\$27.0014

To supply its demands, the studied EH may use three inputs; power from grid, NG from NG network and PV power. There exists at least one connection between any input node to each of electric, thermal and cooling demands. To supply electric demand, EH can either use the purchased electric power or feed the purchased NG into FC and use the generated power of FC. To supply thermal demand, EH can either feed NG into FC or boiler and use their produced thermal power or feed electric power to EHP and use it in heating mode. To supply cooling demand, EH can either feed electric power into EHP and use it in cooling mode, or feed the heat produced by boiler/FC/EHP into absorption chiller and use its produced cooling power. The mentioned redundant connections between input nodes and demands increase the flexibility of EH and reduce its operation cost.

In the studied EH, NG price has a flat price of 3 cents/kWh, however, there exists a TOU tariff for the electricity imported from grid. The price of electricity at off-peak, mid-peak and peak hours are respectively 3 cents/kWh, 6 cents/kWh and 10 cents/kWh. In boiler, with efficiency of 0.85, 1 kWh NG, which costs 3 cents, produces 0.85 kWh heat. This means that boiler produces heat with cost of $\frac{3}{0.85} = 3.5294$ cents/kWh; on the other hand, in FC 1 kWh NG, which costs 3 cents, produces 0.45 kWh power and 0.3 kWh heat.

As per the results, the schedule of EH components and imported energy carriers is mainly affected by the efficiency/COP of components, time variations of demands and energy carriers' prices. At hour 1, in terms of the dispatch of electric power resources, the maximum possible power, i.e. 400 kW is purchased from grid at a price as low as 3 cents/kWh; 5% of this power is lost in transformer and 380 kW is injected into EH. 265.862 kW NG is purchased from NG network, 163.389 kW of which is fed into FC to produce 73.525 kW electric power, PV produces nothing, 30 kW is used to produce ice in CSS, 12.199 kW is used to charge EV batteries, 40 kW is used to charge BSS, $\frac{110}{3.5} = 31.43$ kW is fed into EHP and $283.248 \text{ kW} + 56.6496 \text{ kW} = 339.8976$ kW is consumed by electric demand, as 56.6496 kW shift-up occurs in electric demand.

At hour 1, in terms of the dispatch of the thermal power resources, the mentioned 163.389 kW NG fed into FC produces 49.01 kW thermal power, 58.823 kW NG fed into boiler produces 50 kW thermal power, EHP produces 110 kW heat, absorption chiller consumes $\frac{45}{0.75} = 60$ kW heat, TSS is charged with 11.1725 kW and thermal demand consumes $114.87 \text{ kW} + 22.974 \text{ kW}$, as 22.974 kW shift-up in thermal demand occurs at this low-demand hour. At hour 1, in terms of the dispatch of the cooling power resources, absorption chiller produces 45 kW cooling power and supplies $40.02 \text{ kW} + 4.98 \text{ kW}$ cooling demand, as 4.98 kW shift-up occurs in cooling demand at such a low cooling demand time. From the perspective of NG dispatch, at this hour, $\frac{73.525}{0.45}$ kW of the mentioned 265.862 kW purchased from NG network is fed into boiler and the remaining 43.65 kW supplies NG demand of EH.

According to Fig.2, the share of NG and power in EH purchase significantly changes over time. At low demand hours 1-5 when the electricity price is as low as 3 cents/kWh, the maximum possible power i.e. 400 kW is purchased from grid and NG is the marginal resource of energy. At hours 6-9, maximum power is purchased from both power grid and NG network. At hours 10 and 11 when TOU electricity tariff is at its mid-peak hours, NG is the cheaper energy resource and the maximum possible NG is purchased and the power purchased from grid is the marginal resource of energy. At hours 12-14 when electricity price reaches its peak and coincides with the maximum power generation of PV unit, EH drastically reduces its power purchase in order to reduce its operation cost; the purchased power is reduced from 394.4293 kW at hour 11 to 80.956 kW at hour 12, 75.2208 kW at hour 13 and 120.8265 kW at hour 14.

At hour 15, due to the decrease in PV power, EH operator is forced to increase its purchase from power grid, so that the maximum possible electric power is purchased from grid. At hours 15-21, at most of the times (except for power at 18), the maximum possible power and NG are purchased from power grid and NG network. At hour 22, electricity price is at its peak, so NG is the cheaper resource of energy and the maximum possible NG is purchased, while power purchased from grid is the marginal resource of energy. At hour 23, the price of electricity

suddenly drops from 10 cents/kWh to 3 cents/kWh and power gets the cheaper resource of energy and maximum possible power is purchased. At hour 24, due to low demands, EH purchases low amounts of energy carriers. An important point on the schedule of EH components is variations in operation mode of EHP over time. Its ability to change its operation mode is effective in reducing EH operation cost. At low cooling demand hours such as 1-2 and 21-24, EHP is not necessary to be used in cooling mode, as absorption chiller is sufficient to supply cooling demand. At hours 3-20, EHP is operated in its cooling mode and supplies cooling demand, as absorption chiller is shut-down at hour 4.

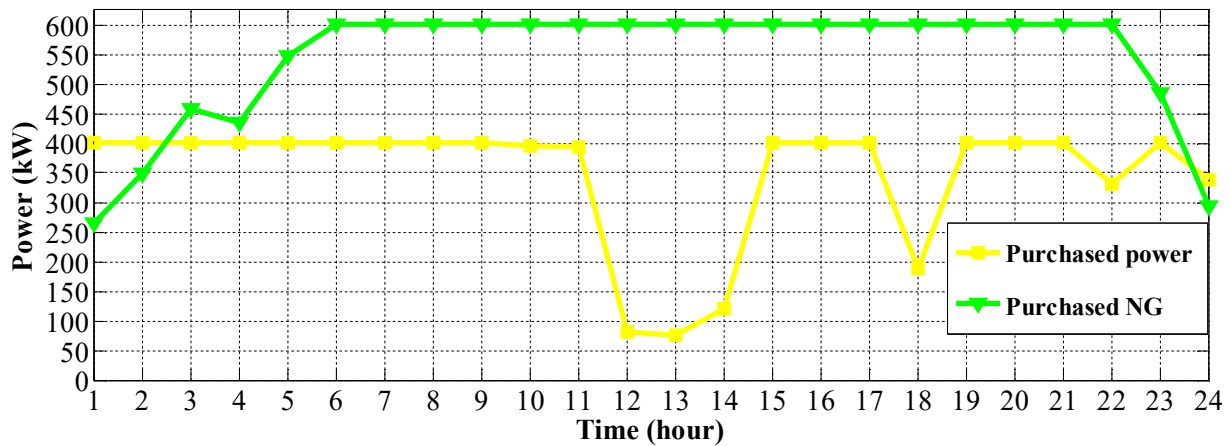


Fig.2. Imported energy carriers

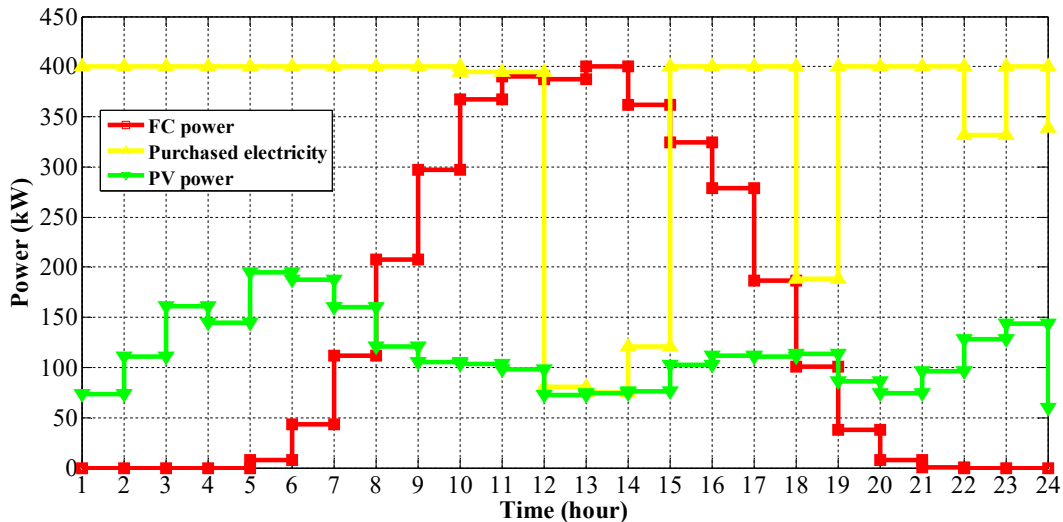


Fig.3. Schedule of electric power resources

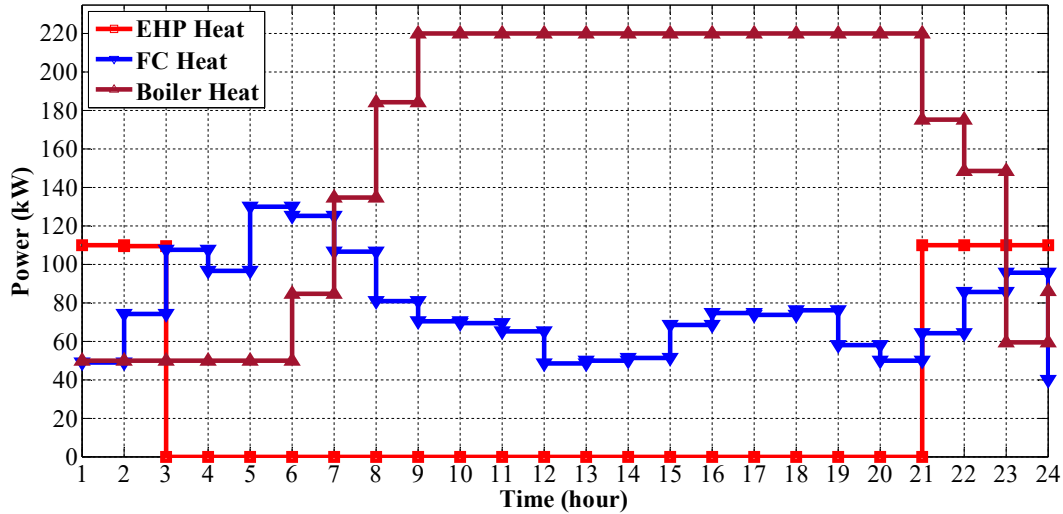


Fig.4. Schedule of thermal power resources

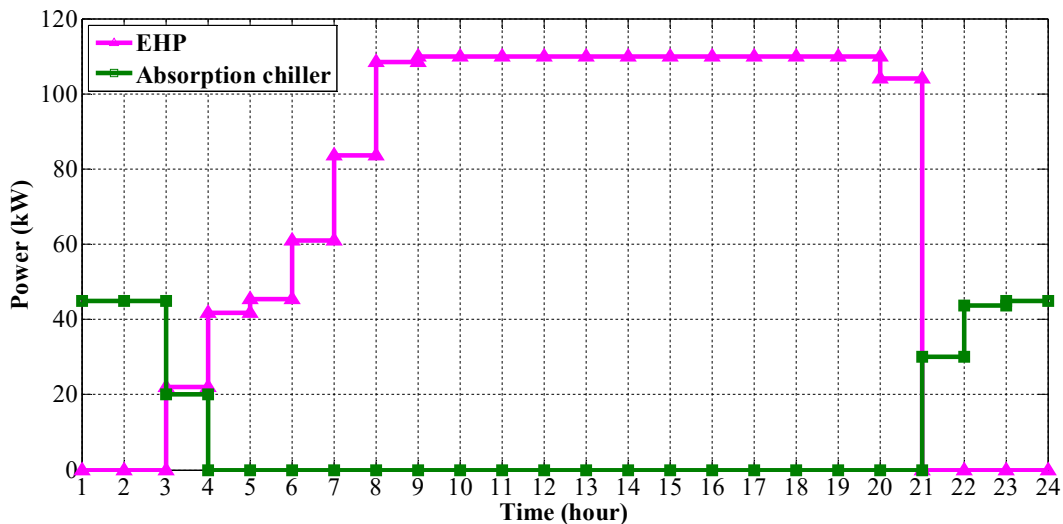


Fig.5. Schedule of cooling power resources

According to figures 6-8, storage systems are charged at times with lower demands and lower electricity prices and are discharged at times with higher demands and prices; so they decrease the operation cost of EH. Due to the coupling among electric, thermal and cooling components, the increase in price of each energy carrier may increase the cost of supplying all forms of energy demands. As per Fig.6, ESS is charged at low demand and low electricity price hours 1-5, is discharged at hour 8, is charged at hour 15 and is discharged at peak price hour 21. As per Fig.7, TSS is charged at low thermal demand hours 1-5 and 7 and then is discharged at hours 10-13 with higher thermal demands. As per Fig.8, CSS is charged at low electric demand hours 1, 5, 10, 16 and 20 and is

discharged at hours 12-15, 18 and 21-23 with higher cooling demands. It must be noted that electric power charges CSS; that is why it is charged at hours with low electric demand.

It must be noted that in the studied EH, due to the consideration of storage loss and degradation costs, in most of the times, storage systems are operated in idle mode. It is expected that the ignorance of storage loss and degradation cost significantly increases the number of charge and discharge of storage systems.

According to Table 5, the batteries of available electric vehicles are charged at low electricity demand and price hours 1-7, when electricity demand is at least 30% less than its peak and electricity price is as low as 3 cents/kWh. In this table, “Ch” and “Dch” respectively signify the charging and discharging modes of EV batteries. EV batteries are discharged at hour 18, when electricity price is 6 cents/kWh and electricity demand reaches its peak and at hours 19-21 with peak electricity price and high electricity demand. Through their charge at low electricity demand and price hours and discharge at high electricity demand and price hours, EV batteries reduce the operation cost of EH.

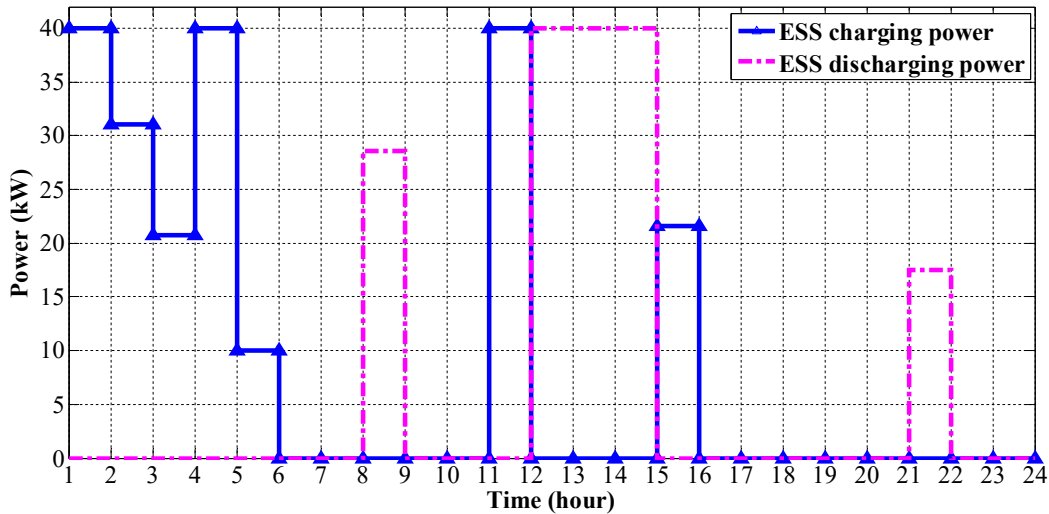


Fig.6. Charging and discharging power of ESS

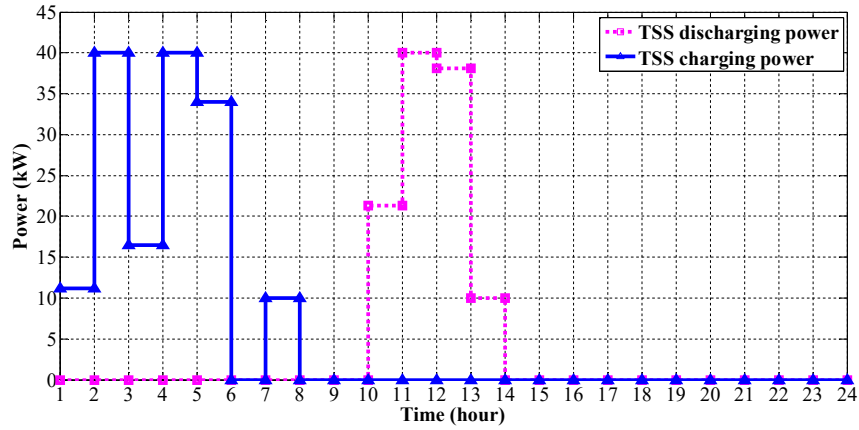


Fig.7. Charging and discharging power of TSS

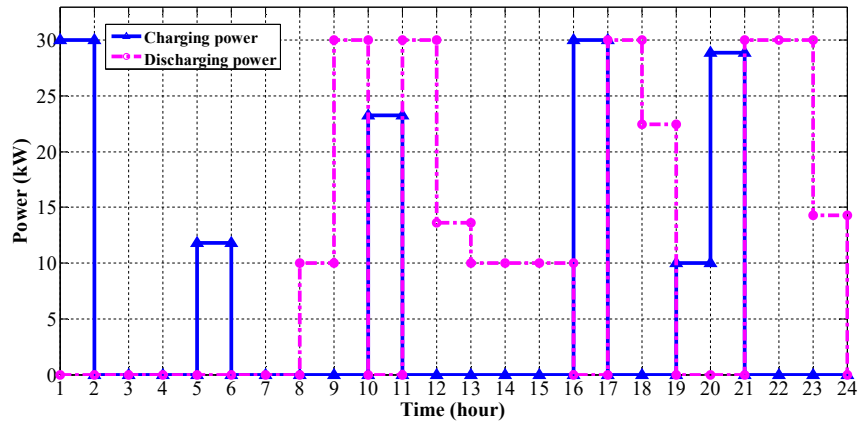


Fig.8. Charging and discharging power of CSS

Table 5. Charging/discharging mode and power of EV batteries

Hour	EV1	EV2	EV3	EV4	EV5	EV6	EV7	EV8	EV9	EV10	EV11	EV12
1	Idle	Idle	Idle	Idle	Idle	Idle	Idle	12.199 Ch	Idle	Idle	Idle	Idle
2	10 Ch	Idle	Idle	Idle	Idle	40 Ch	Idle	Idle	40 Ch	Idle	Idle	Idle
3	30.716 Ch	10 Ch	40 Ch	Idle	27.530 Ch	Idle	40 Ch	Idle	Idle	Idle	Idle	40 Ch
4	Idle	36.769 Ch	Idle	33.502 Ch	Idle	Idle	Idle	Idle	Idle	40 Ch	40 Ch	Idle
5	10 Ch	Idle	10.604 Ch	17.347 Ch	27.530 Ch	10.994 Ch	10 Ch	38.092 Ch	10.994 Ch	10.21 Ch	19.513 Ch	10.604 Ch
6	10 Ch	Idle	10 Ch	Idle	27.530 Ch	10 Ch	10.598 Ch	10 Ch	10 Ch	10 Ch	Idle	10 Ch
7	Idle	14.226 Ch	Idle	10 Ch	Idle	Idle	Idle	Idle	Idle	Idle	Idle	Idle
8	Idle	Idle	Idle	Idle	Idle	Idle	Idle	Idle	Idle	Idle	Idle	Idle
9	Idle	Idle	Idle	Idle	Idle	Idle	Idle	Idle	Idle	Idle	Idle	Idle
10	Idle	Idle	Idle	Idle	Idle	Idle	Idle	Idle	Idle	Idle	Idle	Idle
11	Idle	Idle	Idle	Idle	Idle	Idle	Idle	Idle	Idle	Idle	Idle	Idle
12	Idle	Idle	Idle	Idle	Idle	Idle	Idle	Idle	Idle	Idle	Idle	Idle
13	Idle	Idle	Idle	Idle	Idle	Idle	Idle	Idle	Idle	Idle	Idle	Idle
14	Idle	Idle	Idle	Idle	Idle	Idle	Idle	Idle	Idle	Idle	Idle	Idle
15	Idle	Idle	Idle	Idle	Idle	Idle	Idle	Idle	Idle	Idle	Idle	Idle
16	Idle	Idle	Idle	Idle	Idle	Idle	Idle	Idle	Idle	Idle	Idle	Idle
17	Idle	Idle	Idle	Idle	Idle	Idle	Idle	Idle	Idle	Idle	Idle	Idle
18	10 Dch	13.636 Dch	Idle	Idle	Idle	19.757 Dch	33.133 Dch	10 Dch	32.929 Dch	33.133 Dch	32.501 Dch	33.133 Dch
19	Idle	29.935 Dch	10 Dch	24.321 Dch	10 Dch	Idle	10 Dch	Idle	Idle	10 Dch	10 Dch	10 Dch
20	32.575 Dch	Idle	32.477 Dch	18.924 Dch	32.477 Dch	Idle	Idle	32.575 Dch	Idle	Idle	Idle	Idle
21	Idle	Idle	Idle	Idle	Idle	22.782 Dch	Idle	Idle	10 Dch	Idle	Idle	Idle

22	Idle	Idle	Idle	Idle	Idle	Idle	Idle	Idle	Idle	Idle	Idle	Idle
23	Idle	Idle	Idle	Idle	Idle	Idle	Idle	Idle	Idle	Idle	Idle	Idle
24	Idle	Idle	Idle	Idle	Idle	Idle	Idle	Idle	Idle	Idle	Idle	Idle

Figures 9-11 indicate that demand response shifts a portion of demand from times with higher demands and energy carriers' prices to the times with lower demands and energy carriers' prices so that EH operation cost is decreased. As per Fig. 9, at hours 1-11 shift-up occurs in electric demand; within this time interval, at hours 1-7 and 10-11, the maximum possible shift-up occurs in electric demand which means that at these hours, the maximum demand response participation constraint performs as a binding constraint and with higher maximum demand response participation factor, lower EH operation cost could be achieved. At peak electricity price hours 12,13 and14, when electric demands are also high, the maximum shift-down in electric demand occurs. Moreover, at hours 18-22 with peak electricity prices, the maximum possible shift-down occurs in electric demand.

According to Fig.10, at low thermal demand hours 1-9 and 21-24, shift-up occurs in thermal demand and at higher thermal demand hours 11-20, shift-down of thermal demand occurs. At hours 1-7 and 22-24, the maximum possible shift-up occurs for thermal demand. As per Fig.11, at low cooling demand hours 1-9, shift-up occurs in cooling demand and at hours 2-8, the maximum possible shift-up occurs for cooling demand.

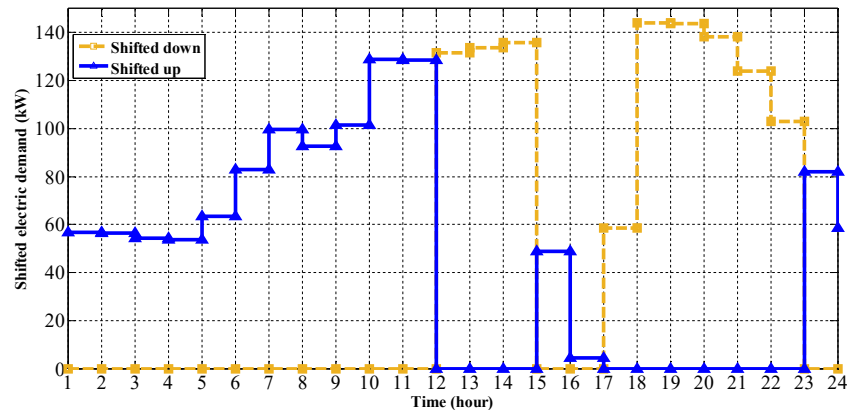


Fig.9. Electric demand to be shifted at different hours

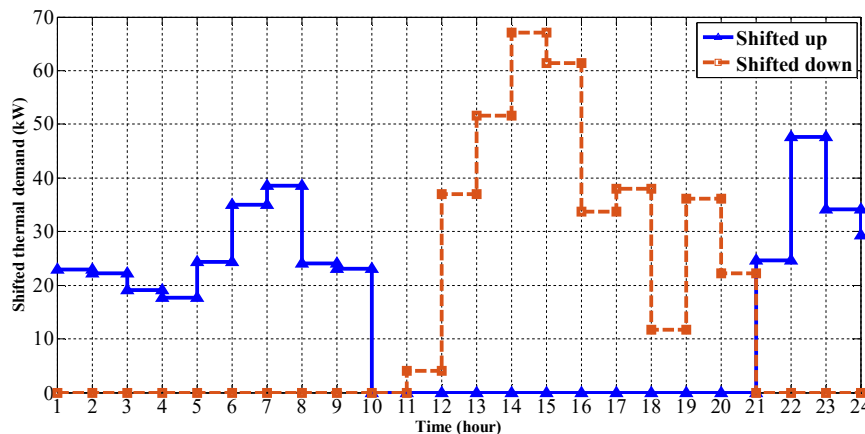


Fig.10. Thermal demand to be shifted at different hours

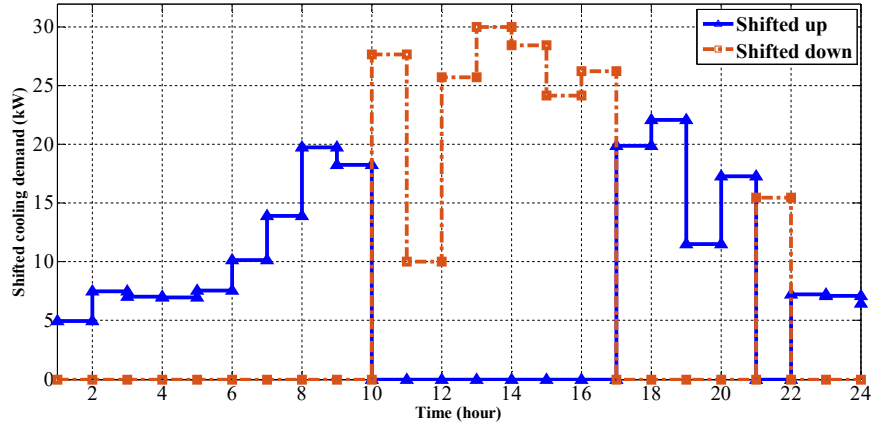


Fig.11. Cooling demand to be shifted at different hours

3.2. Stochastic EH scheduling

In this case, the uncertainties of electric, thermal, NG and cooling demands and also the uncertainty of initial energy level of EV batteries arrived at parking lot, are considered and the stochastic UC is done for EH. In the proposed stochastic UC model, introduced in section 2, the expected operation cost of EH is minimised. The number of uncertain input data is 132. Forecast error of all data has been assumed 5% and they are modeled as Gaussian PDF. 3000 initial scenarios are created and Scenred module in GAMS has been used to reduce the number of scenarios to 10. The probabilities of the reduced scenarios are tabulated as Table 6. Generated and reduced scenarios for electric, thermal, cooling and NG demands, PV power and initial EV battery levels have been respectively illustrated as figures 12-17. The initially generated scenarios are in red and the reduced scenarios are in green. There exists no interdependence between different sets of uncertain input data.

Table 6. Probability of reduced scenarios

Scenario number	1	2	3	4	5	6	7	8	9	10
Probability	0.083	0.093	0.100	0.110	0.106	0.092	0.135	0.068	0.113	0.101

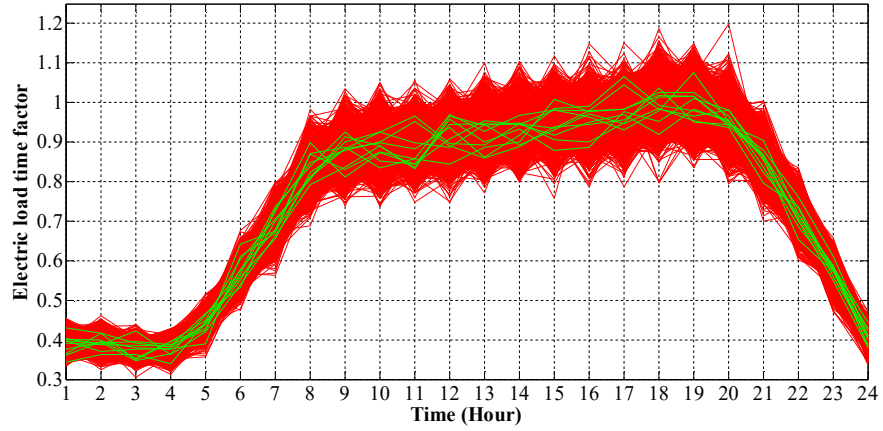


Fig.12. Generated and reduced scenarios for electric load

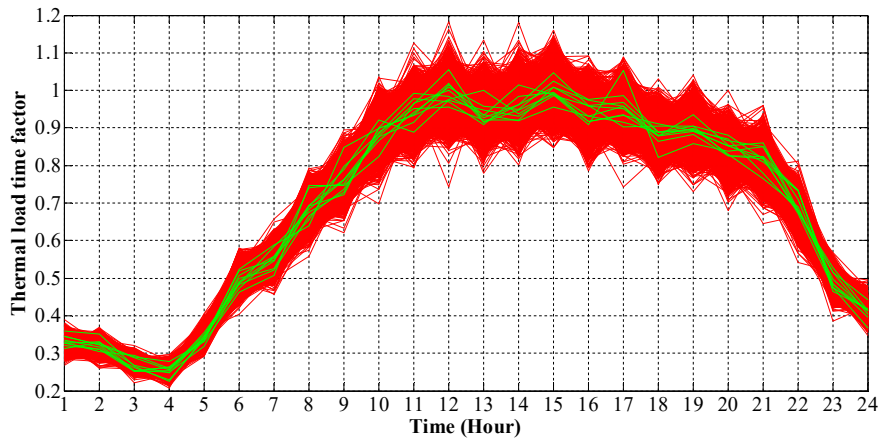


Fig.13. Generated and reduced scenarios for thermal load

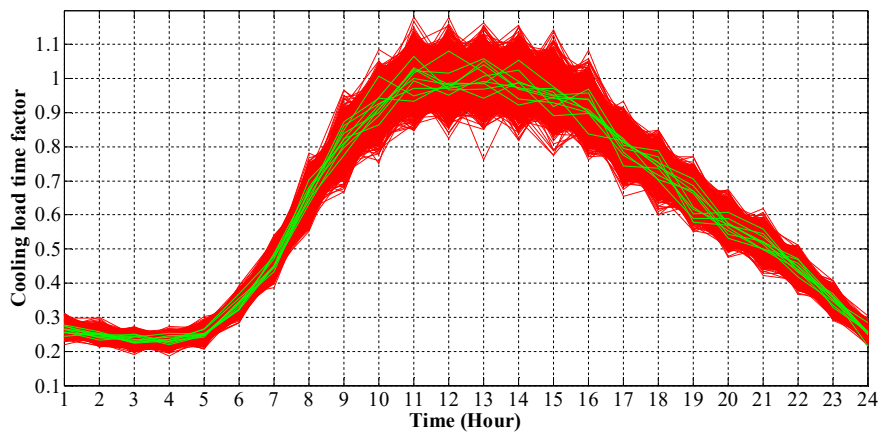


Fig.14. Generated and reduced scenarios for cooling load

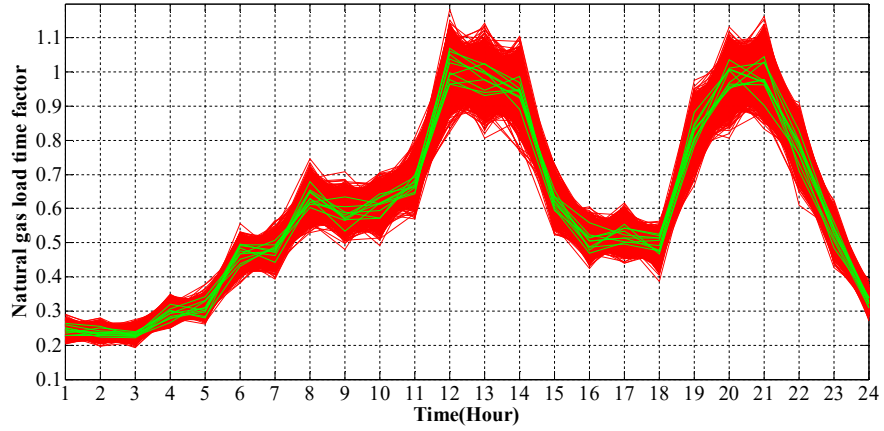


Fig.15. Generated and reduced scenarios for NG load

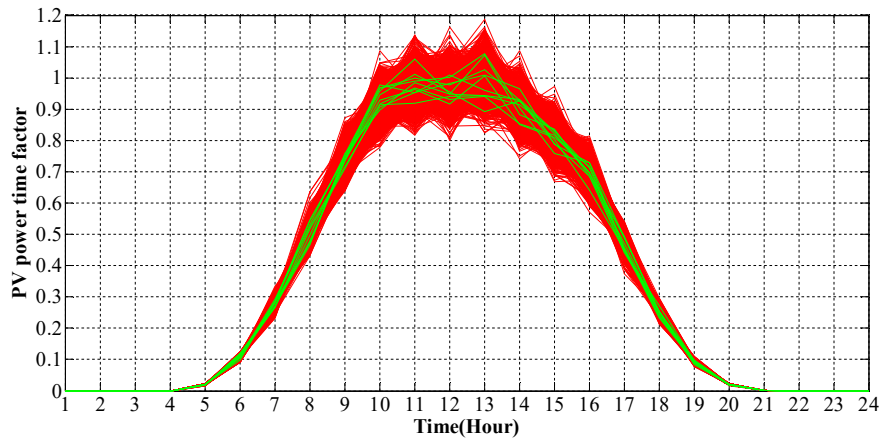


Fig.16. Generated and reduced scenarios for PV power

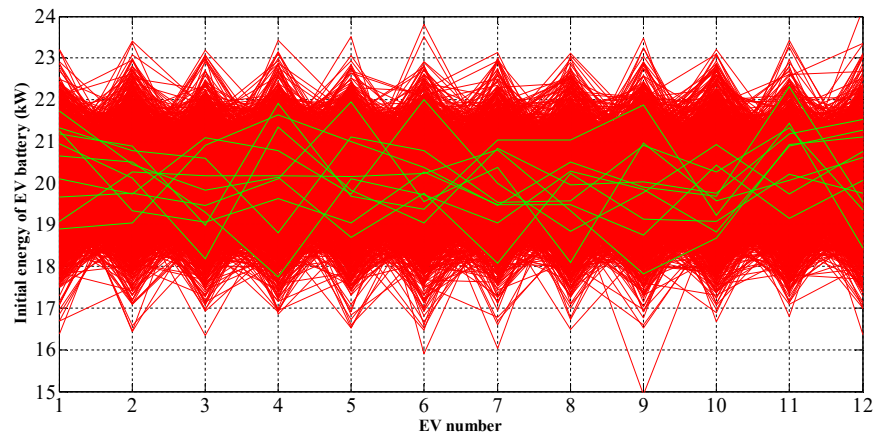


Fig.17. Generated and reduced scenarios for initial energy level of EV batteries

It must be noted that stochastic model, due to its very high number of decision variables and constraints, is not trivial to be solved. With resource limits of 500 and 60, the achieved expected operation cost with CPLEX solver was respectively \$896.7690 and \$902.0478. With 3000 as resource limit, CPLEX achieved \$895.7073 as the expected EH operation cost. The achieved expected operation cost is a bit lower than EH operation cost, when the uncertainties were ignored, i.e. \$896.5105. Each scenario has its own operation cost and there is the risk of experiencing higher operation costs than expected operation cost at different scenarios. Higher severity of uncertainties increases the risk of high operation costs. The expected values of operation cost components can be found in Table 7.

Table 7. Expected values of operation cost components (\$)

EH operation cost	895.7073	CSS degradation cost	0.507
Cost of purchased electricity	458.770	Total storage degradation cost	2.743
Cost of purchased NG cost	391.899	EV batteries degradation cost	6.301
Total load shed cost	2.272	Electric DR cost	21.948
Total start up/shut down cost	7.007	Thermal DR cost	3.763
ESS degradation cost	1.905	Cooling DR cost	1.003
TSS degradation cost	0.331	Total DR cost	26.715

3.3. Effect of EV fleet and storage systems on EH operation

In this subsection, first the effect of EV fleet and the number of EVs on EH operation cost is investigated. As per subsection 3.1, with the fleet of 12 EVs, EH operation cost was \$896.5105. The results show that without EV fleet, EH operation cost would be as high as \$974.7496 which means that EV batteries decrease EH operation cost by \$78.2391, i.e. 8%. EV batteries are charged at low demand and low electricity price hours and on the other hand inject electric power into EH at hours with high demand and electricity prices through their V2G capability; in this way, EVs reduce the operation cost of EH.

An important question is how the number of EVs affects EH operation cost. Does the increase in number of EVs necessarily results in lower EH operation cost? Is there an optimal number of EVs in the parking lot? The results, illustrated as Fig.18, shows that the increase in the number of EVs in the parking lot does not necessarily decreases EH operation cost and also show that 20 is the optimal number of EVs. A sharp decrease in EH operation cost occurs when the number of EVs is increased from 0 to 1, 1 to 2 and 2 to 3. EH operation cost decreases from \$974.7496 in the case without EV fleet to \$944.6318 with 1 EV, \$921.5801 with 2 EVs and \$909.5085 with 3

EVs. However, with further increase in the number of EVs, less decrease in EH operation cost is seen. Increasing the number of EVs beyond 20 not only does not decrease EH operation cost, but also increases it. Such an increase in EH operation cost is due to the excessive losses and degradation of EV batteries. With 20 EVs, EH operation cost would be as low as \$892.4876.

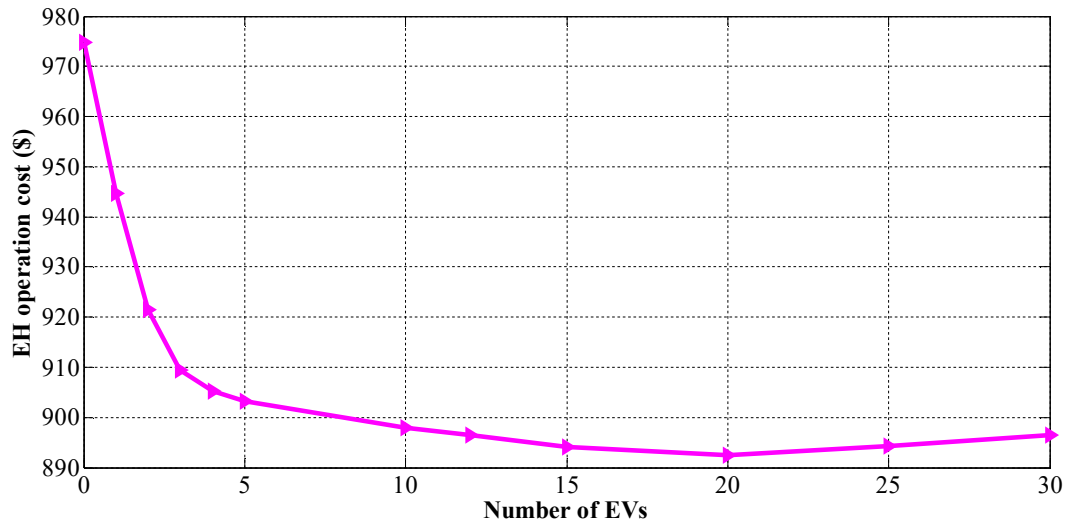


Fig.18. EH operation cost versus number of EVs

Here, in order to investigate the effect of different storage systems, i.e. ESS, TSS and CSS on EH operation, EH operation cost has been determined for different combinations of storage systems and the results have been illustrated as Fig. 19. The effect of different storage systems on EH operation cost mainly depends on their size, total charge/discharge capacity, replacement cost, charge/discharge/storage efficiencies, demand profiles, price profiles of energy carriers as well as EH architecture and components. As per the results, the operation cost of EH without any storage system is as high as \$1019.2436. The results also show that the addition of ESS decreases EH operation cost by only 0.26%, while TSS and CSS decrease EH operation cost respectively by 5% and 10.7%. Therefore, TSS and then CSS have significant effect on reduction of EH operation cost, while the effect of ESS is trivial. The low effect of ESS is due to the fact that in the absence of ESS, EV batteries do what it could do; they are charged at low demand and price hours and inject their stored energy to EH at high demand and price hours through V2G capability; in other words, there is an overlap between the performance of ESS and EV batteries.

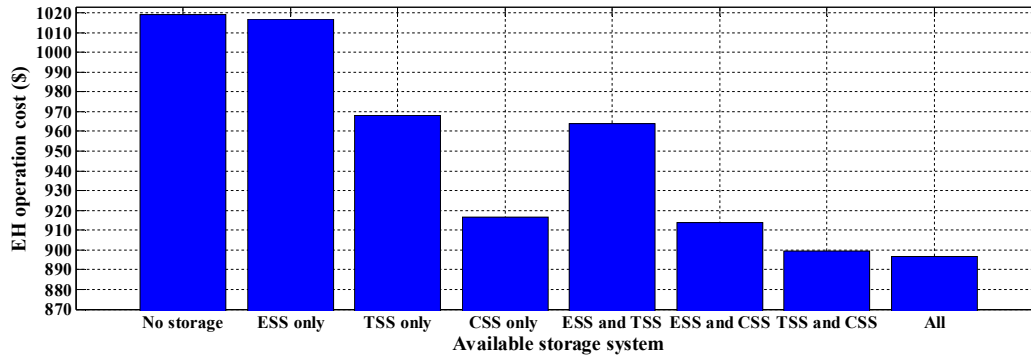


Fig.19. Effect of storage systems on EH operation cost

3.4. Effect of DR and DR participation factor on EH operation

In this subsection, first the effect of different DR programs on EH operation is investigated. The results, illustrated as Fig. 20, indicate that DR programs collectively decrease EH operation cost by 26.9%. The results also indicate that thermal DR is more effective than electric DR and cooling DR; as it decreases EH operation cost by 12%, while electric DR and cooling DR decrease EH operation cost respectively by 9.3% and 4.2%. An important point is that the effect of responsive demands and storage systems is somehow similar, as both attempt to mitigate the fluctuations of renewable resources, decrease the utilisation factor of less efficient components and increase the utilisation factor of more efficient components and flatten the load profiles.

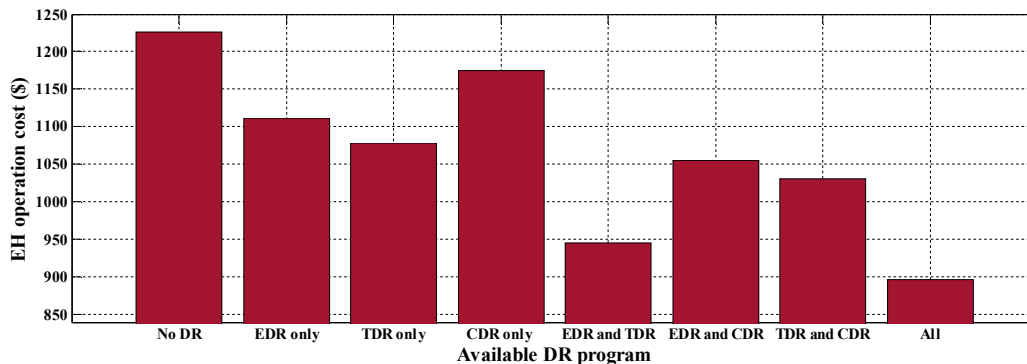


Fig.20. Effect of DR on EH operation cost

Here, the effect of electric/thermal/cooling demand participation factor on EH operation is investigated. EH operation cost versus electric, thermal and cooling demand participation factors have been respectively illustrated as figures 21, 22 and 23. Fig.21 shows that at low electric demand participation factors (EDPFs), a small increase in EDPF sharply decreases EH operation cost. For instance, with increase of EDPF from 0 to 0.01, the decrease in operation cost is as big as 2.3% or increase of EDPF from 0 to 0.05 decreases operation cost decreases by 10%. However, 10% increase in EDPF from 0.4 to 0.5 decreases the operation cost by only 0.5%. Figures 22 and 23 show that the changes in EH operation cost versus thermal demand participation factors and cooling demand participation factors are very similar to Fig.21.

At low thermal demand participation factors (TDPFs), a small increase in TDPF sharply decreases EH operation cost. For instance, with 10% increase of TDPF from 0 to 0.1, operation cost decreases by 10.6%, however, 10% increase in TDPF from 0.4 to 0.5 decreases the operation cost by only 0.5%. At low cooling demand participation factors (CDPFs), a small increase in CDPF significantly reduces EH operation cost; with 10% increase of CDPF from 0 to 0.1, operation cost decreases by 3%, however, 10% increase in CDPF from 0.4 to 0.5 decreases the operation cost by only 0.17%.

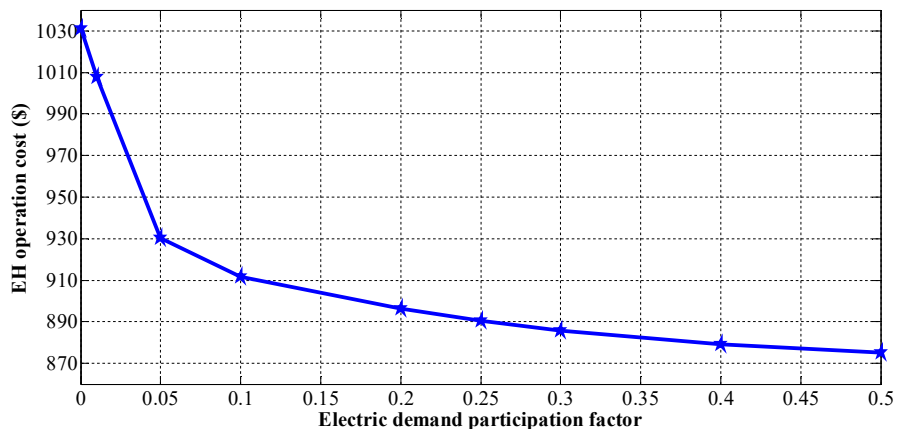


Fig.21. Effect of EDPF on EH operation cost

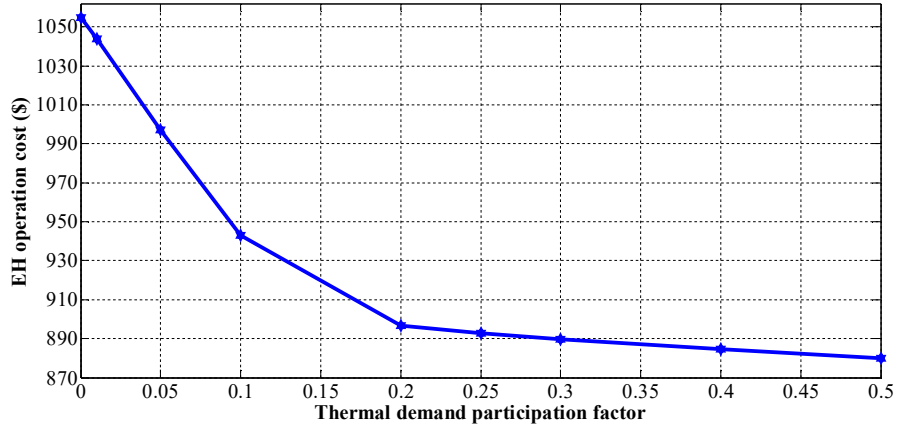


Fig.22. Effect of TDPF on EH operation cost

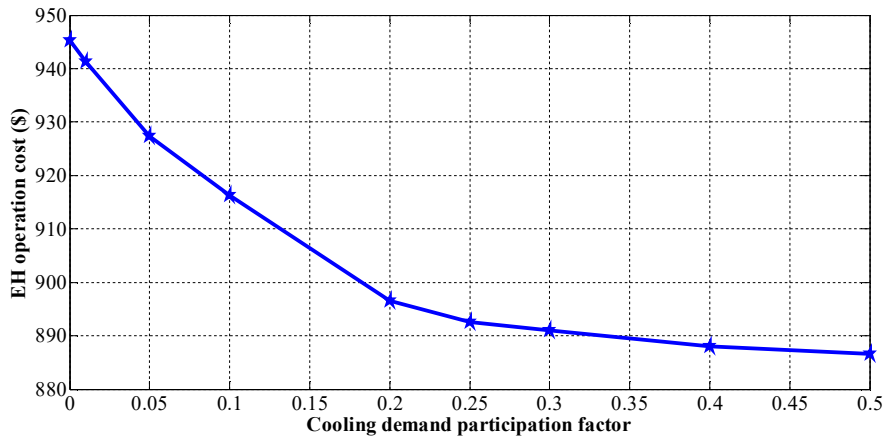


Fig.23. Effect of CDPF on EH operation cost

4. Conclusions and future work

In this paper, a new stochastic model has been developed for unit commitment in EHs including an intelligent EV parking lot, boiler, PV unit, FC, EHP, absorption chiller, electric/thermal/cooling storage systems, electricity and NG as input energy carriers and electricity, heat, cooling and NG demands. The uncertainties of demands, PV power and initial energy level of EV batteries have been modeled with MCS and the charge/discharge/storage loss and degradation of storage systems and EV batteries have been considered. The effect of demand response and demand participation factors as well as effect of storage systems and EVs on EH operation has been investigated.

The results imply that thermal demand response is more effective than electric demand response and cooling demand response; as it decreases EH operation cost by 12%, while electric demand response and cooling demand response decrease it respectively by 9.3% and 4.2%. The results show that at low electric/thermal/cooling demand

participation factors, an increase in participation factor sharply decreases EH operation cost, while at higher participation factors, that increase leads to a lower decrease in operation cost. For instance, with 10% increase of thermal demand participation factor from 0 to 0.1, operation cost decreases by 10.6%, however, its 10% increase from 0.4 to 0.5 decreases the operation cost by only 0.5%. The results show that thermal storage system and then cooling storage system have significant effect on reduction of EH operation cost, while the effect of electric storage system is minor. The results show that the increase in the number of EVs in the parking lot does not necessarily decreases EH operation cost and also show that 20 is the optimal number of EVs. A sharp decrease in EH operation cost occurs when the number of EVs is increased from 0 to 1, 1 to 2 and 2 to 3. EH operation cost decreases from \$974.7496 in the case without EV fleet to \$944.6318 with 1 EV, \$921.5801 with 2 EVs and \$909.5085 with 3 EVs, however further increase in the number of EVs leads to smaller reduction in EH operation cost. As a direction for future research, developing more realistic models for EH components as well as experimental validation is recommended.

Conflict of interest

The authors declare that there is no conflict of interest for this paper.

Acknowledgement

J.P.S. Catalão acknowledges the support by FEDER funds through COMPETE 2020 and by Portuguese funds through FCT, under POCI-01-0145-FEDER-029803 (02/SAICT/2017).

References

- [1] M. Geidl, G. Koepfel, P. Favre-Perrod, B. Klöckl, G. Andersson, K. Fröhlich, The energy hub—a powerful concept for future energy systems, in: *Third annual Carnegie mellon conference on the electricity industry*, 2007, pp. 14.
- [2] A. Najafi, A. Tavakoli, M. Pourakbari-Kasmaei, M. Lehtonen, A Risk-based Optimal Self-Scheduling of Smart Energy Hub in the Day-ahead and Regulation Markets, *Journal of Cleaner Production*, (2020) 123631.
- [3] M. İnci, M. Büyük, M.M. Savrun, M.H. Demir, Design and analysis of fuel cell vehicle-to-grid (FCV2G) system with high voltage conversion interface for sustainable energy production, *Sustainable Cities and Society*, 67 (2021) 102753.
- [4] M. İnci, Active/reactive energy control scheme for grid-connected fuel cell system with local inductive loads, *Energy*, 197 (2020) 117191.

- [5] İ. Mustafa, Design and modeling of single phase grid connected fuel cell system, in: 2019 4th International Conference on Power Electronics and their Applications (ICPEA), Ieee, 2019, pp. 1-6.
- [6] A.R. Jordehi, How to deal with uncertainties in electric power systems? A review, *Renewable and sustainable energy reviews*, 96 (2018) 145-155.
- [7] F. Zhu, J. Fu, P. Zhao, D. Xie, Robust energy hub optimization with cross-vector demand response, *International Transactions on Electrical Energy Systems*, (2020) e12559.
- [8] M.S.J. A. Rezaee Jordehi, João P. S. Catalão, Dynamic economic load dispatch in isolated microgrids with particle swarm optimisation considering demand response, in: *IEEE UPEC*, IEEE, Torino, Italy, 2020.
- [9] K. Afrashi, B. Bahmani-Firouzi, M. Nafar, IGDT-Based Robust Optimization for Multicarrier Energy System Management, *Iranian Journal of Science and Technology, Transactions of Electrical Engineering*, (2020) 1-15.
- [10] H. Hosseinnejad, S. Galvani, P. Alemi, Optimal Probabilistic Scheduling of a Proposed EH Configuration Based on Metaheuristic Automatic Data Clustering, *IETE Journal of Research*, (2020) 1-23.
- [11] M.-W. Tian, A.G. Ebadi, K. Jermsittiparsert, M. Kadyrov, A. Ponomarev, N. Javanshir, S. Nojavan, Risk-based stochastic scheduling of energy hub system in the presence of heating network and thermal energy management, *Applied Thermal Engineering*, 159 (2019) 113825.
- [12] A. Soroudi, A. Keane, Risk averse energy hub management considering plug-in electric vehicles using information gap decision theory, in: *Plug in electric vehicles in smart grids*, Springer, 2015, pp. 107-127.
- [13] M. Vahid-Pakdel, S. Nojavan, B. Mohammadi-Ivatloo, K. Zare, Stochastic optimization of energy hub operation with consideration of thermal energy market and demand response, *energy Conversion and Management*, 145 (2017) 117-128.
- [14] A. Mansour-Saatloo, M. Agabalaye-Rahvar, M.A. Mirzaei, B. Mohammadi-Ivatloo, M. Abapour, K. Zare, Robust scheduling of hydrogen based smart micro energy hub with integrated demand response, *Journal of Cleaner Production*, 267 (2020) 122041.
- [15] A. Najafi-Ghalelou, S. Nojavan, K. Zare, B. Mohammadi-Ivatloo, Robust scheduling of thermal, cooling and electrical hub energy system under market price uncertainty, *Applied Thermal Engineering*, 149 (2019) 862-880.
- [16] F. Brahman, M. Honarmand, S. Jadid, Optimal electrical and thermal energy management of a residential energy hub, integrating demand response and energy storage system, *Energy and Buildings*, 90 (2015) 65-75.
- [17] F. Jamalzadeh, A.H. Mirzahosseini, F. Faghihi, M. Panahi, Optimal operation of energy hub system using hybrid stochastic-interval optimization approach, *Sustainable Cities and Society*, 54 (2020) 101998.
- [18] S. Mansouri, A. Ahmarinejad, M. Ansarian, M. Javadi, J. Catalao, Stochastic planning and operation of energy hubs considering demand response programs using Benders decomposition approach, *International Journal of Electrical Power & Energy Systems*, 120 (2020) 106030.
- [19] A.R. Jordehi, Particle swarm optimisation with opposition learning-based strategy: an efficient optimisation algorithm for day-ahead scheduling and reconfiguration in active distribution systems, *Soft Computing*, (2020) 1-18.